Hindawi
International Journal of Antennas and Propagation
Volume 2023, Article ID 2843443, 36 pages
https://doi.org/10.1155/2023/2843443

Review Article

Structural-Electromagnetic-Thermal Coupling Technology for Active Phased Array Antenna

Pengying Xu,[1] **Yan Wang**,[2] **Xiaoxian Xu**,[1] **Longyang Wang**,[1] **Zhihai Wang**,[3] **Kunpeng Yu**,[3] **Wenzhi Wu**,[3] **Meng Wang**,[4] **Guojun Leng**,[5] **Dongming Ge**,[6] **Xiaofei Ma**,[7] **and Congsi Wang**[8]

[1]*Key Laboratory of Electronic Equipment Structure Design, Ministry of Education, Xidian University, Xi'an 710071, China*
[2]*School of Information and Control Engineering, Xi'an University of Architecture and Technology, Xi'an 710055, China*
[3]*China Electronics Technology Group Corporation No. 38 Research Institute, Hefei 230088, China*
[4]*Shaanxi Huanghe Group Co. Ltd., Xi'an 710043, China*
[5]*China Electronics Technology Group Corporation No. 29 Research Institute, Chengdu 610036, China*
[6]*Beijing Institute of Spacecraft System Engineering, Beijing 100094, China*
[7]*Xi'an Institute of Space Radio Technology, Xi'an 710100, China*
[8]*Guangzhou Institute of Technology, Xidian University, Guangzhou 510555, China*

Correspondence should be addressed to Yan Wang; wangyan5169@163.com and Congsi Wang; congsiwang@163.com

Received 2 April 2022; Revised 30 May 2022; Accepted 3 March 2023; Published 17 March 2023

Academic Editor: Giuseppe Castaldi

Active phased array antenna (APAA) is a representative of complex electronic equipment, and it plays significant roles in scenarios such as battlefield situation perception, aviation guidance, and communication. It has become the core equipment in land, navigation, and aeronautical applications. With the continuous improvement of technical changes and military requirements, the working frequency band, pointing accuracy, gain, and low sidelobe level of APAA increase, and the multidisciplinary design contradiction between antenna electrical performance and structure and temperature becomes increasingly prominent. As a result, the electrical performance of APAA in service is prone to be affected by the external complex environments. The structural-electromagnetic-thermal (SET) coupling problem has become a key problem restricting the development of APAA. This paper has summarized the structural features and environmental loads of advanced APAA on different platforms and provided design basis and principle for antenna designer. And then the SET coupling theory of APAA has been introduced, which can be applied in both the design and manufacturing stage, as well as the performance control technology in service environment of APAA. This theory helps to analyze the impact of environmental factors, such as antenna structure deformation, radome high-temperature ablation, and feed errors, on the antenna's performance. For 128×768 spaceborne array antenna, in the range of 25~85°C, the gain of antenna decreases with the increase of operating temperature and decreases by 0.015 dB with each increase of 1°C. The key design parameters in the fields of antenna manufacturing accuracy, efficient heat dissipation, and lightweight design are also analysed; for 32×32 rectangular planar phased array antenna, the gain of antenna decreases by 2.715 dB when the random error of installation position in x, y, and z direction reaches 1/10 of the wavelength. In addition, condition monitoring, displacement field reconstruction, and electrical performance compensation of APAA have also been touched to help engineers maintain and guarantee the antenna performance throughout its life cycle. Finally, the future research direction of SET technology of APAA has been discussed, and SET technology is extended to more fields such as antenna parameter uncertainty, high-frequency circuit electronics manufacturing, and electronic equipment performance guarantee.

1. Introduction

Since 1960s, the emergence of phased array technology has led to significant military changes and quickly become the mainstream form of modern radar [1–3]. Active phased array radar (APAR), with the advantages of fast scanning speed, multi-function, multi-target tracking, high reliability, and strong anti-jamming ability, has become the core equipment in the fields of warplane early warning, fire control, missile guidance, satellite imaging, strategic missile early warning, and other national defense fields [4–7]. However, the unpredictable battleground condition will seriously affect the overall performance of APAR. Meanwhile, with the development of APAA towards high performance, high frequency band, and high integration, it turns out to be a closer coupling relationship between structure design, device thermal power consumption, and electromagnetic performance. Multi-field structural-electromagnetic-thermal coupling has become one of the key problems restricting the development of APAR [8–12].

As shown in Figure 1, APAA in service will undergo various environmental loads such as wind, rain and snow, solar radiation, and random vibration. These loads will directly affect the displacement field and temperature field of antenna structure. Deformation of the array structure will cause the element to offset from its ideal position and deviate from the normal direction of antenna array at certain angle direction. The change of temperature field will cause thermal deformation of structure on the one hand and temperature drift of electronic device performance on the other hand. Changes in temperature and displacement fields directly or indirectly affect the electrical performance of the antenna. APAA design parameters, such as the rigidity of the array structure, will be limited by the load-bearing capacity and array antenna lightweight requirements. Array antenna heat dissipation design will be affected by the space of heat dissipation, density of the powerful component, and the form of heat dissipation. The results of these different design parameters also affect the displacement field, temperature field, and electromagnetic field of the array antenna. The structural displacement field, electromagnetic field, and temperature field of APAA have mutual influence, which will be affected by service environment and also restrict the main design parameter selection of APAA. In APAA, the interaction and influence of the electromagnetic field, structural displacement field, and temperature field are common issues. ① The structural design parameters, such as antenna bearing frame and radio frequency components, affect the structural displacement field and electromagnetic field. ② The service environment will change the antenna displacement field and temperature field, thus restricting the design optimization of the antenna structure such as lightweight and heat dissipation. ③ The change of temperature field directly affects the performance of electronic devices such as T/R module and antenna electromagnetic field. ④ The high thermal power consumed by tens of thousands of T/R components will change the temperature field, which will affect the displacement field of the antenna structure and then the electromagnetic field. ⑤ As a boundary condition, displacement field directly affects temperature field and electromagnetic field. ⑥ High-power electromagnetic fields will affect the temperature field and signal transmission performance through electromagnetic induction. The abovementioned coupling relationships will affect the service performance of APAA. Military applications have an increasingly higher detection power of APAA, so it is necessary to study the SET coupling. Numerous research studies have been devoted to the performance assurance of APAA on various platforms under a certain service loading [13–18]. Meanwhile, relevant experimental verification has been conducted and remarkable results have been achieved. In order to improve the performance of APAA, some researchers [19, 20] have summarized many significant advantages of metamaterial (MTM) and metasurface (MTS), which play an important role in upgrading the next generation of wireless communication systems. Other researchers [21, 22] have summarized the application of metamaterial (MTM), metasurface (MTS), and substrate integrated waveguide (SIW) in millimeter-wave (mmWave) and terahertz (THz) high-performance on-chip antenna. In addition, it is also an effective method to improve the performance of the array antenna by changing the shape of the radiation element [23, 24]. At the same time, circular polarized antennas are well suited for long-distance transmission attainment. Some studies have made good summaries on the research progress of APAA on different platforms. However, the application fields of different military electronic equipment are quite different, and different requirements are put forward for APAA. It is urgent to conduct a comparative analysis on the characteristics of APAA of different platforms [25–29]. Therefore, this paper first describes the main performance indexes and technical characteristics of advanced APAA on different carrier platforms, then analyses the characteristics and impacts of service environment loads on different platforms, introduces the theory of SET coupling and its application in the design, manufacture, and service performance regulation of APAA, and finally discusses the development trend of APAA and the future research directions of the SET coupling technology.

2. Development Trends of APAA

Phased array technology first appeared in the late 1930s, and the United States pioneered the study. In the 1960s, the United States and the former Soviet Union have developed and equipped several phased array radars, mostly for ballistic missile defense systems. In the 1970s, phased array radar developed rapidly. In addition to the United States and the Soviet Union, many countries started to develop and equip phased array radar, such as China, Britain, France, Japan, Italy, Germany, and Sweden. In this period, APAA has the characteristics of high mobility, miniaturization of antenna, diversification of antenna scanning system, and wide application range. In the 1980s, the application scope of phased array radar was further extended because of its unique advantages. Meanwhile, the multi-functional phased array radar was widely used in the new generation of medium and

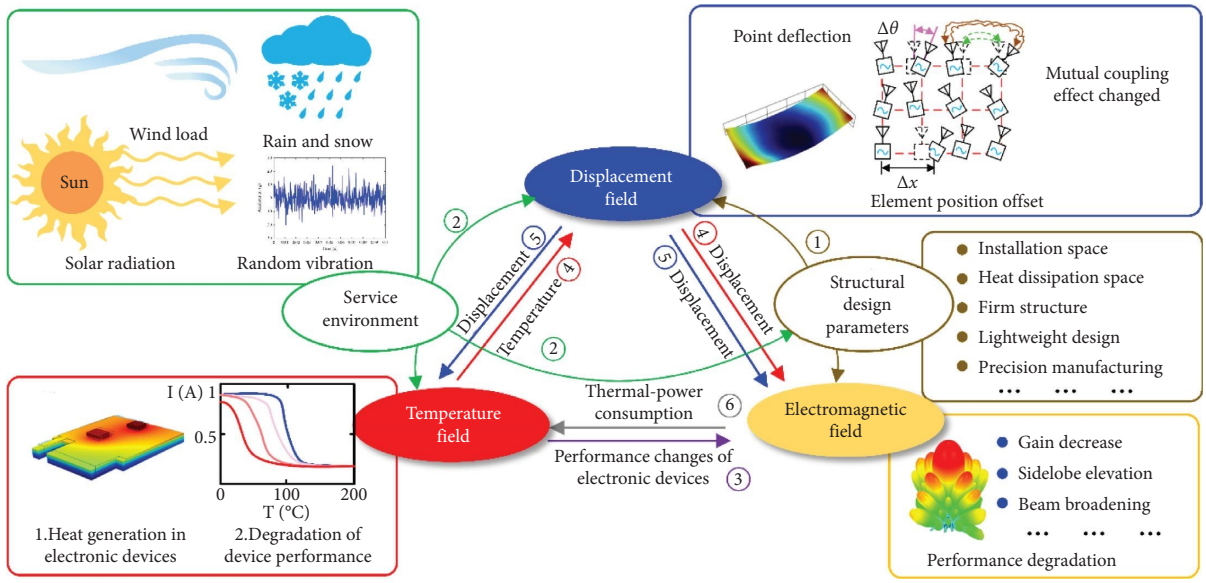

Figure 1: Structural-electromagnetic-thermal coupling relationship of APAA.

long-range air defense missile weapon systems. This is an important symbol of the third generation of medium and long-range air defense missile weapon systems, and the operational performance of the weapon system was greatly improved. Since the 1990s, countries all over the world have continuously furthered the research of APAA and have developed APAA for the fighter, warship, missile, satellite, and other platforms, meeting the requirements of modern war for the weapon system. As shown in Figure 2, an advanced APAA plays a significant role in the five-dimensional modern war of land, sea, air, space, and information. Nowadays, countries all over the world are constantly developing new technologies to improve the detection power of radar [13].

As shown in Figure 2, modern warfare has completed the transformation from the plane mode connected by land and sea to the three-dimensional mode of land, sea, and air. The five-dimensional integrated new multi-dimensional combat mode of land, sea, air, and space has fundamentally changed the traditional three-dimensional battlefield space. The coordinated detection of different radar networks on land, sea, air, and space and the fusion of multi-source information in the battlefield can achieve high-quality information acquisition and then guide weapons and equipment to implement three-dimensional air superiority and interception operations. The main manifestations are as follows. The development of high-performance radar and long-range strike weapons has greatly expanded the combat space, and the plane dimension of the battlefield can spread to any corner of the Earth. A variety of detection capabilities, strike power, combat forms, and destruction methods can be applied and imposed almost simultaneously in a small combat space. In this way, various types of weapons and equipment distributed in a wide space can form an instantaneous huge and devastating blow in a specific space. At the same time, the new space has introduced high-tech confrontation. Electronic warfare competes in the electromagnetic space. Electronic countermeasure reconnaissance, electronic interference, and electronic defense are playing an increasingly important role in the modern battlefield.

2.1. Ground-Based. As an important part of the anti-missile system, ground-based strategic early-warning radar is an advanced equipment for the country. Figure 3 shows the world's advanced ground-based radar (GBR) and vehicle-mounted anti-stealth radar.

AN/FPS-85 [3] is the world's first large phased array radar, and it works in UHF band, and the radar consists of 5,134 transmitters and 4,660 receivers, with a total output power of 32 MW. It is reported that it is the only phased array radar having the capability of tracking deep-space orbiting satellites. The antenna array is 97 m long and 43.5 m high and covers an area of 23,225.76 m^2. The weight of the steel structure is up to 1,250 tons. AN/FPS-108, "Cobra Dane" [3], has a large fixed phased array with a diameter of about 30 m and working band of L band. It consists of 34,768 elements, of which 15,360 are active radiating elements with a peak power of up to 920 kW. The AN/FPS-115 "Pave Paws" [3] is used in the detection and warning of submarine-launched ballistic missiles and satellite tracking systems. Its work frequency ranges from 420 to 450 MHz, and the detection distance can reach 4,800 km. It consists of a pair of circular planar phased arrays with a diameter of about 30 m, which are mounted on adjacent sides of building with array dip angle of 20° and a height of about 32 m. Each side of the radar uses 1,792 T/R modules, the synthesized beam coverage of the two arrays covers a pitch angle of 85° and an azimuth angle of 240°, and the peak power of each array is 580 kW. The AN/TPY-2 radar as the "Eye of THAAD" is a key part of the terminal high altitude area defense (THAAD) system [30]. The APAA area of AN/TPY-2 is 9.2 m^2, the number of T/R modules is 25,334, the peak power of the elements can reach 16 W, and

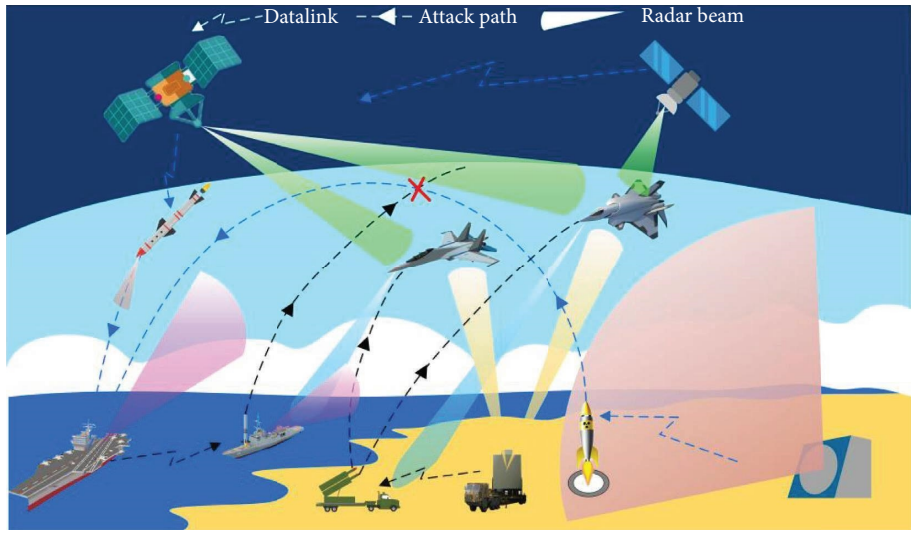

Figure 2: Five-dimensional modern war of sea, land, air, sky, and information.

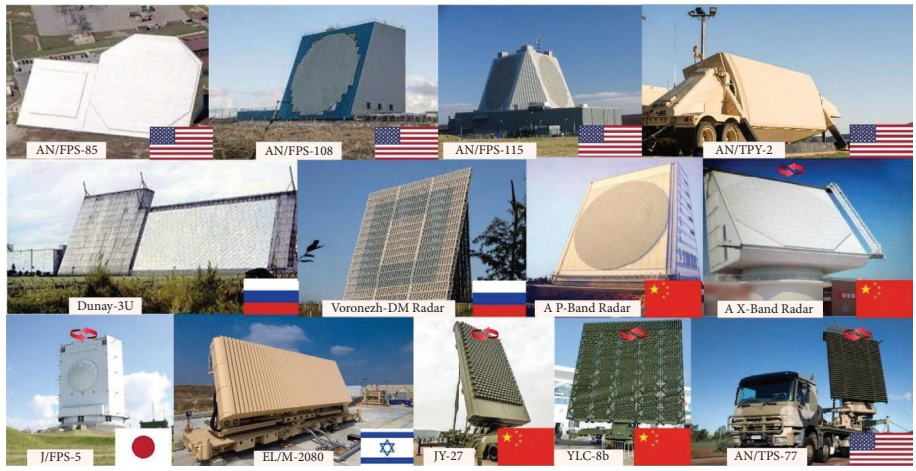

Figure 3: Typical GBR and vehicle-mounted anti-stealth radar in the world.

the average power of APAA is about 60 kW~80 kW. The detection distance of the radar is up to 2,300 km, and the target detection distance of the 1 m^2 radar cross section (RCS) is 1,700 km. Dunay-3U [31] was built in 1978 and works in the UHF band. This antenna has 30 waveguides, each of which has been excited by a separate 100 kW transmitter. The area of the receiving antenna is 5,000 m^2. Voronezh-DM [31], Russia's latest generation of early warning radar, provides long-distance watching of airspace to prevent ballistic missile attacks and aircraft surveillance and was put into operation in 2009. Designed by NPK NIIDAR and working in the UHF band, it has a detection range of 10,000 km and can track 500 targets at the same time. In 2017, China first publicly demonstrated a P-band long range early-warning phased-array radar with a detection distance of 500 km. Since the electromagnetic band absorbed by stealth coating used by the stealth aircraft is mostly in the range of 0.3 GHz~29 GHz, the working frequency of the meter-wave radar just avoids the stealth band of the stealth aircraft, so the meter-wave radar "naturally" has the specialty of discovering the stealth aircraft. In 2018, A large X-band multi-target measurement APAR was first exposed in China, which can achieve full space coverage detection by rotation of the antenna over 360° in azimuth. Rotating phased array radar has electronically scanning capability both in pitch and azimuth, which makes it more flexible to allocate resources compared with traditional mechanical scanning radar. Rotating phased array radar has lower manufacturing costs and energy consumption than fixed radar, which used three or four arrays to cover the entire detection area. The radar has a detection range of about 4,000 km for a target of 10 m^2. Japanese J/FPS-5 [32] is manufactured by Mitsubishi Electric, used to detect and track aircraft, cruise missiles, and ballistic missiles. The system is installed on a hexagonal structure that stands at a total height of 34 meters. Three of the hexagonal structure's large sides are equipped with antennae, each ranging in diameter from 12 m to 18 m. The largest of APAA works in S-band. The remaining two-sided APAR is about 12 m in diameter and works in the L-band. The structure can rotate

on a circular rail in order to track continuously in whole area without blind zone, as necessary to point the radar in a highly threatening direction. EL/M-2080 "Green Pine" [33] is an Israeli ground-based missile defense radar produced by Elta. It works in UHF band, with 2,000~2,300 T/R modules, and weighs about 60 tons. It can work in search, detection, tracking, and missile guidance modes simultaneously, detect targets with a range of about 500 km, and track more than 30 targets at a speed of 3,000 m/s, and the missile can be guided within 4 m of the target.

In order to satisfy the multi-task and multi-function requirements of the new generation of 3D radars, a phased array antenna capable of flexible scanning in azimuth and pitch is required. This 2D electronically scanning phased array antenna is mounted on a rotating antenna pedestal and rotates mechanically over a range of 360 degrees in azimuth. Therefore, in any azimuth position, the antenna beam can perform high-speed phased scanning in certain azimuth and pitch ranges. More flexibility is provided to achieve energy management of radar signals. YLC-8B [34] mobile APAR is the fourth-generation air defense early warning detection radar developed by China. YLC-8B works in UHF band, which is given due attention to the stealth aircraft threat in the modern warfare in its development process. JY-27 APAR is China's VHF-band stand-off surveillance, capable of discovering U.S. stealth aircraft with a detection air target distance of 500 km. AN/FPS-77 [35] is a 3D air search APAR produced by Lockheed Martin in 1980. The APAA consists of 1,156 solid-state T/R modules and uses gallium nitride (GaN) technology with improved performance, while prolonging the operational life and reduced life cycle costs. The APAA works in L-band, with a detection range of 370~460 km, and a large number of pencil beams are generated when working. Table 1 summarizes the comparison of the main parameters of typical ground-based radars in the world.

2.2. Shipborne. In modern naval warfare, the main threat faced by warships is the attack from all kinds of weapons in the air. In order to effectively solve the threat of multi-directional, multi-batch saturated attack from air and sea to surface fleet under complex electromagnetic interference environment, the APAR has been developed successively by navies around the world.

Nimitz Class and USS America under the U.S. Navy are equipped with AN/SPS-48E [36], which is a large, long-range, and three-coordinate air defense radar with strong air search and tracking capabilities to deal with possible air threats. The radar is manufactured by ITT Exelis, working in S or E/F band, peak power is 2.4 MW, and the maximum detection distance is 426 km. Antenna array size is $5.48 \times 5.33\ m^2$; the APAA is arranged from 95 linear array elements and weighs about 2578 kg and can operate in extremely harsh environment. U.S. Navy Aegis system is one of the world's most advanced ship-board combat systems. The heart of the Aegis system is its powerful radar system: AN/SPY-1 [37]. AN/SPY-1 works in S-band and consists of four antenna arrays, each of which is covering 90° and about $3.65 \times 3.65\ m^2$ in size, and has a total transmission power of 4 MW~6 MW, and the detection airspace range is 320 km~480 km. Sejong the Great-class destroyer developed in South Korea, Atago class under the Japanese Maritime Self-Defense Force, and Hobart class destroyer of the Royal Australian Navy are all equipped with the Aegis Shield system. The AN/SPY-3 designed by Raytheon Corporation in the United States is the first shipborne multi-functional APAR of the U.S. Navy [38]. AN/SPY-3 is an advanced X-band APAR with three APAAs, each with an antenna size of $2.72 \times 2.08\ m^2$, a thickness of 0.635 m, and a total weight of 2.5 tons. Each antenna array consists of 5000 T/R modules and 8 T/R modules form a fast-dismantling transmit-receive integrated multi-channel module (TRIMM) with a maximum search distance reaching up to 320 km. DDG1000 is a guided-missile destroyer of the United States Navy, equipped with AN/SPY-3 APAR. The AN/SPY-4 [39] is another APAR designed by Raytheon, which consists of three APAAs with an array antenna size of $4.06 \times 3.86\ m^2$ and thickness of 0.76 m, the total weight of three antennas is 10.215 tons, and it has an effective detection distance of more than 463 km. Gerald R Ford Class was equipped with AN/SPY-3 and AN/SPY-4 APAR to improve its ocean survival and strike capabilities. Like AN/SPY-3/AN/SPY-4, AN/SPY-6 [40] has a radar modular assembly (RMA) consisting of multiple T/R modules. AN/SPY-6, equipped with Arleigh Burke class, works in S-band with four-sided APAA, each consisting of 37 RMA and more than 5,000 T/R modules. With GaN materials, the power of each T/R module can be greatly increased. Admiral Kuznetsov is a conventionally powered aircraft carrier of the Russian Navy. The main radar is a 4-sided "Sky Watch" multi-functional APAR [41], and it has 5,100 T/R modules per plane. Its working frequency band is 0.2 GHz~4 GHz, ranging from UHF band to S-band. At present, the long-range searching radar equipped on the major European frigate is SMART-L [42] APAR. The APAA is installed in a large 8 m long frame with 24 antenna arrays working in L band and 132 kW peak power, capable of fully automatic detection, tracking up to 1000 targets over a 400 km range. The latest large aircraft carrier of the Royal Navy, Queen Elizabeth-class, the French large destroyer Horizon class, and the British Type-45 Daring class all carry SMART-L radar. Liaoning is China's first serving aircraft carrier, carrying 346 type "Sea Star" radar [43], which is a highly digitized and multi-functional APAR, working in S-band. The radar has 5,000 T/R modules on each side and a detection distance of more than 450 km and can detect and track 100 targets. The 052 C destroyer is the first domestic vessel in the Chinese Navy equipped with four-sided APAR and 346 type APAR. 346A uses a more efficient liquid cooling method, which greatly enhances the detection distance, anti-jamming, and power of the radar. Currently, 346A is mainly installed on China's most important warship 052D. 346B is an enlarged version of 346A, mostly installed on the latest serviced 055 destroyer. After carrying this type of radar, the detection distance jumped to more than 40 km, and the integrated operation ability rose to a new level. The main parameters of typical shipborne radars in the world are compared in Table 2.

Table 1: Main parameters of different GBR.

Country	Radar	Frequency band	Quantity of T/R modules	Detection distance (km)	Peak power
USA	AN/FPS-85	UHF	5,134 transmitters 4,660 receivers	40,744	32 MW
	AN/FPS-108	L	15,360	46,000	920 kW
	AN/FPS-115	UHF	1,792×2	4,800	580 × 2 kW
	AN/TPY-2	X	25,334	2,300	60~80 kW
Russia	Dunay-3U	VHF	30 waveguides	300~4500	500 kW
	Voronezh-DM	UHF	NR	8000	0.7 MW
China	P-band radar	P	NR	500	NR
	X-band radar	X	NR	4000	NR
	JY-27	VHF	512	500	NR
	YLC-8b	UHF	1650	700	NR
Japan	J/FPS-5	S	NR	460	NR
Israel	EL/M-2080	L	NR	500	NR

NR: not reported.

Table 2: Main parameters of different shipborne radar.

Country/region	Radar	Frequency band	Quantity of T/R modules	Detection distance (km)	Peak power
USA	AN/SPS-48E	E and F bands	NR	460	35 kW
	AN/SPY-1	S	4,736	370	6 MW
	AN/SPY-3	X	NR	320	NR
	AN/SPY-4	S	NR	463	NR
	AN/SPY-6	S	NR	324	NR
Russia	Sky Watch	UHF~S	5,100	324.1	NR
Europe	SMART-L	L	NR	400	132 kW
China	Type 346	S	5,000	450	125 kW

NR: not reported.

2.3. Airborne. Advanced fighters are of great significance to a country's national defense and national science technology, especially in the territorial air defense and the expulsion of intrusion aircraft. Its strategic significance cannot be replaced by other military equipment [44]. Airborne APAA is one of the most advanced fire control radars in the world. This paper lists the 10 most advanced fighters in active service in the world and their advanced APAR, as shown in Figure 4.

The F-35 Lightning II [45] is a single-seat, single-engine, all-weather stealth multi-role combat fighter designed and manufactured by Lockheed Martin, equipped with an AN/APG-81 APAA. The F-35 is mainly used for front-line support, target bombing, air defense interception, and other tasks. It belongs to the fifth-generation fighter and has a high stealth design, advanced electronic system, and supersonic cruise capability. The F-22 Raptor [45], jointly developed by Lockheed Martin and Boeing, is a single-seat, twin-engine, fifth-generation, extremely advanced tactical fighter equipped with AN/APG-77 APAA. The combination of stealth, sensitivity, accuracy, and situation awareness makes the F-22 the world's best comprehensive performance fighter today. F/A-18 E/F Super Hornet is a single-seat, single-engine, supersonic versatile fighter developed by Boeing for the U.S. Navy and equipped with AN/APG-79 APAR. It is mainly used for maritime air defense and also for ground attack. McDonnell Douglas F-15E Strike Eagle [45] is a two-seat, twin-engine, supersonic fighter with ground attack as its main mission. It is equipped with AN/APG-63(V3) APAA and has the ability of ground attack and air superiority. It is called a dual mission fighter.

Eurofighter Typhoon [46] is a versatile fourth-generation fighter with twin engines, delta wing, canard configuration, and high maneuverability designed by Eurofighter GmbH. Equipped with Captor-E APAA, the combination of electronic beam scanning and flexible radar resource management can provide excellent detection performance and ensure multi-target tracking, missile guidance, and situational awareness at the same time. Rafale [46] is the fourth-generation fighter with twin engines, delta wing, high maneuverability, and versatility in France. Equipped with RBE-2 APAA, it can track 8 targets at the same time and can automatically evaluate the threat degree of targets and set priorities. The Su-57 is a single-seat, twin-engine, stealth, and versatile heavy-duty fighter of the Russian air force. The avionic equipment of the Su-57 [47] fighter has been qualitatively improved and is no longer the "weakness" of the Russian fighter. Su-57 is equipped with N036 Byelka APAR, which has 5 APAAs. Combined with 2 airborne computers, the system can find targets 400 km away, track 30 air targets and attack 8 of them at the same time. The Su-35 [47] is a fourth-generation aircraft using the

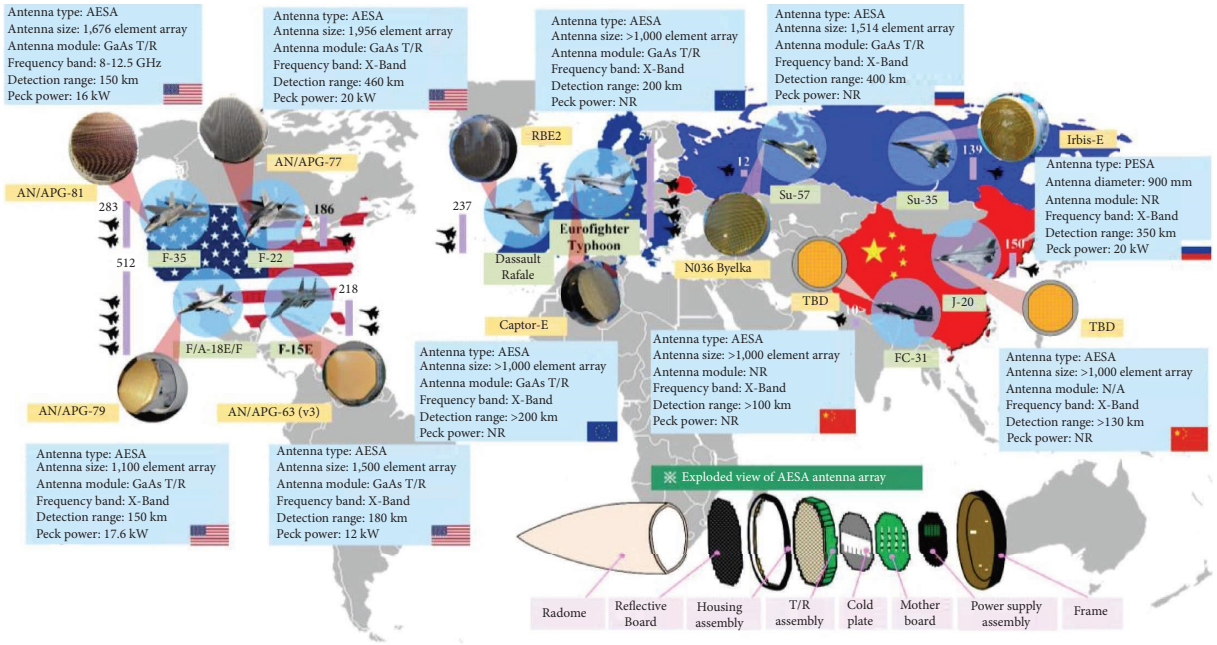

Figure 4: Top 10 most advanced fighters in the world and their APAA.

fifth-generation technology. Equipped with Irbis-E PEAA, it can detect air targets up to 400 km away, track 30 air targets, and engage eight of them at the same time. In addition, the multi-function radar can provide high-resolution ground images using synthetic aperture mode.

Chengdu J-20 [48] is the fifth-generation single-seat, twin-engine, stealth fighter manufactured by Chengdu Aircraft Industry Co., Ltd. It is equipped with advanced APAR, with high stealth, high situation awareness, high maneuverability, and other capabilities. FC-31 [48] is the fifth-generation single-seat, twin-engine, stealth fighter developed by Shenyang Aircraft Corporation. The aircraft has high survivability: low RCS, low infrared radiation characteristics, and excellent electronic countermeasure performance; multi-task capability: strong target detection capability, excellent situation awareness, over-the-horizon multi-target attack, and adaptability to complex weather conditions. Table 3 shows a comparison of the main parameters of typical airborne radar in the world.

2.4. Missile-Borne. Active radar is the mainstream of modern tactical missile radar seeker. The missile does not need to rely on external guidance signals while flying. It uses energy in the most effective route to achieve a longer range or has a higher mobility before hitting the target. Since the end of last century, engineering research on APAA in missile has been carried out all over the world. Table 4 lists the main parameters of different missile-borne radars. The AAM-4B [49], developed by Mitsubishi Electric Co. Ltd. of Japan, is the world's first air-to-air missile equipped with an AESA radar seeker. Its detection ability and anti-electromagnetic interference ability are greatly improved compared with the traditional mechanical scanning radar. The seeker antenna works in Ka-band with a detection distance of 120 km. Based on its phased array electronic scanning feature, it detects and scans predefined space quickly and has a higher target refresh rate. It is especially suitable for targets with high dynamics. The accuracy of parameters such as the electronic tracking angle is also relatively high. In addition, with the development of digital beamforming technology, it can form a variety of beams to deal with multiple targets.

The new K-77M [50] air-to-air missile developed by Russia for Su-57 is guided by a 64-element AESA antenna instead of the traditional planar slot antenna, which can be scanned both electronically and mechanically. This avoids the search range degradation performance of large scan angle for active electronically scanned array radar.

The PL-15 is an active radar-guided long range air-to-air missile developed by the China Guided Missile Institute. The missile features an active electronically scanned array radar seeker and has an alleged range exceeding 200 km. It is 4 meters long and incorporates a dual-thrust solid-fuel rocket motor, capable of a speed of Mach 4.

In addition, the AIM-120 is the advanced medium-range air-to-air missile which is one of the most modern, powerful, and widely used air-to-air missiles in the entire world. Its variant AIM-120D [51] also used AESA instead of mechanical scanning seeker, which provides greater range (about 160 km), better guidance, and a higher kill probability. Italian navy said the new Teseo Mk2/E anti-ship missile will have a new generation AESA (active electronically scanned array)-based seeker as part of the terminal guidance dual mode head section also including an electro-optical sensor for high-precision sea and land target engagements. The Defence Research and Development Organisation of India has incorporated an advanced electronically scanned array (AESA) radar into the nose of the Astra Mk1 missile. This modification enhances the missile's ability to detect targets, as it now has a lock-on

Table 3: Main parameters of different airborne radar.

Country/region	Radar	Frequency band	Quantity of T/R modules	Detection distance (km)	Peak power
USA	AN/APG-81	X	1,676	150	16 kW
	AN/APG-77	X	1,956	460	20 kW
	AN/APG-79	X	1,100	150	17.6 kW
	AN/APG-63 (V3)	X	1,500	180	12 kW
Europe	Captor-E	X	>1000	>200	NR
	RBE-2	X	>1000	200	NR
Russia	N036 Byelka	X	1,514	400	NR
	Irbis-E	X	NR	350	20 kW
China	J-20's radar	X	>1000	>135	NR
	FC-31's radar	X	>1000	>100	NR

NR: not reported.

Table 4: Main parameters of different missile-borne radar.

Country	Missile	Frequency band	Operational range	Maximum speed
Japan	AAM-4B	Ka	120 km	Mach 4~5
Russia	K-77M	NR	400 km	Mach 5
China	PL-15	NR	200~300 km	Mach 4.5
USA	AIM-120D	NR	>160 km	Mach 4

NR: not reported.

range of 13 km for a 5 m^2 RCS target and is capable of live target detection and tracking. Additionally, the missile features a narrow target acquisition beam and a strong electronic counter-countermeasures capability, which improves its ability to launch in lock-on after launch (LOAL) mode. This development represents a significant improvement in the missile's overall performance and effectiveness. The main parameters of typical missile-borne APAA are compared as follows.

2.5. Spaceborne. Spaceborne radar has the capability of all-weather, all-time Earth observation. Moreover, the spaceborne APAA has a very large surveillance area, observing a wide variety of military targets. It can carry out a wide-range and high-resolution surveillance and reconnaissance on the ground and sea battlefields from the air and space and can be used to support the air-to-ground and air-to-sea accurate identification and aiming of fighters. Therefore, it plays an important role in modern warfare. APAA has been successfully applied in synthetic aperture radar (SAR) due to its excellent performance. SAR was first used in the late 1950s on RB-47A and RB-57D strategic reconnaissance aircraft. After nearly 60 years of development, SAR technology has been relatively mature. As shown in Figure 5, each country has established its own development plan for SAR. Various new systems of SAR have emerged and play an important role in civil and military fields.

In 1978, NASA launched the world's first SAR satellite, Seasat-A [53], marking the beginning of the era of SAR Earth observation. Since then, NASA has launched SIR-A, SIR-B, and SIR-C imaging radars into space using space shuttles in 1981, 1984, and 1994, respectively. SAR has gradually developed from the original HH single-polarization and L-band SAR satellites to the radar system with four polarization modes (HH, HV, VV, and VH) and multi-band (L, C, and X). In 1991, Russia launched the Almaz-1 [53] satellite for radar imaging for geophysical, agricultural, geological, and environmental applications. The main sensor is an S-band APAA with a resolution of 10 m~15 m. In terms of radar imaging reconnaissance satellites, Russia launched the new SAR satellite Kondor-E [53] in 2013 with a spotlight resolution of 1 m and a width of 10~20 km; the strip map mode is 1 m~3 m and the width is 10 km~20 km, and the scan mode is 5 m~30 m and the width is 20 km~150 km, and it has 3D observation and interferometry capabilities. In 1991 and 1995, ESA launched the European Remote Sensing Satellite (ERS) series of civil radar imaging satellites, ERS-1 and ERS-2 [53], which work in C-band and VV polarization and are mainly used for imaging land, ocean, glacier, coastline, and others. High-quality images with a spatial resolution of 30 m and an observation bandwidth of 100 km can be obtained. Envisat [53], one of the ESA Earth Observation Satellites, was launched in 2002. The satellite is Europe's largest environmental satellite ever built and the largest equipment on board is the advanced SAR, which generates high-quality, high-resolution images of oceans, coasts, polar ice caps, and land. Envisat-1 is mainly used to monitor the environment and make continuous observations of the Earth's surface and atmosphere for mapping, resource exploration, meteorology, and disaster judgment. Launched in 2014, the Sentinel-1 [54] Earth monitoring satellite carries a 12 m C-band SAR capable of scanning up to 400 km. RadarSat-1 [54] is Canada's first commercial Earth Observation Satellite, which monitors changes in the Earth's environment and natural resources. Working in C-band, it uses HH polarization mode and has 7 beam modes and 25 imaging modes. RadarSat-2 [54] is a new generation of

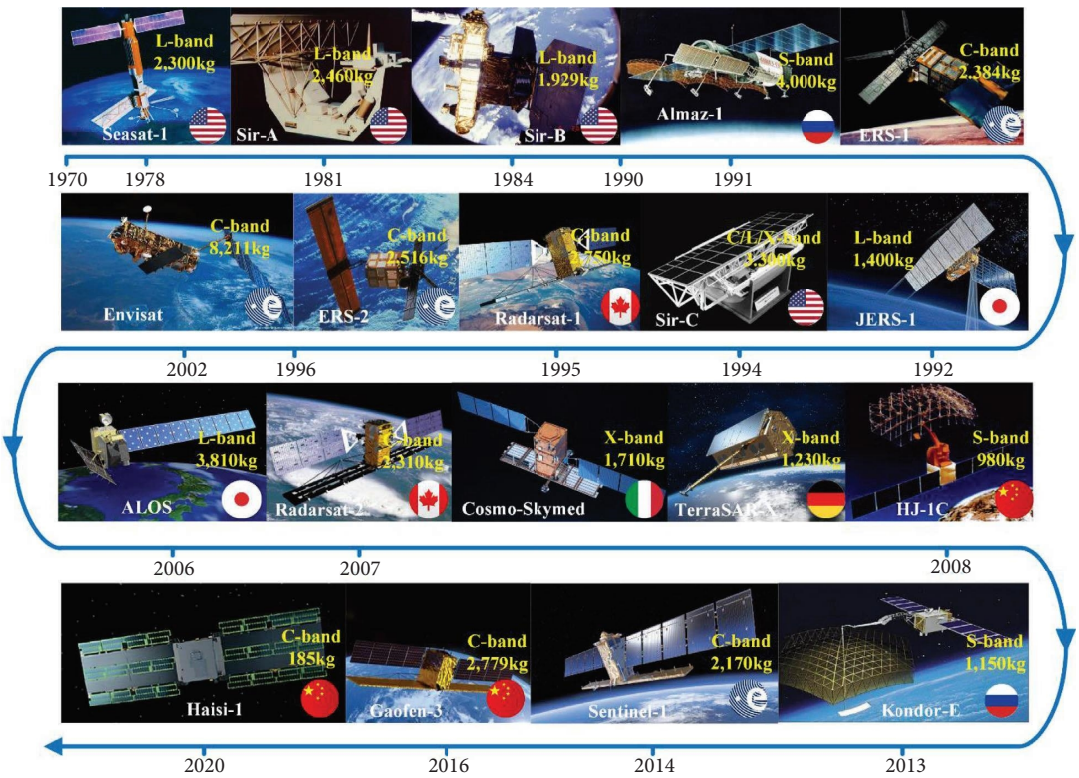

Figure 5: Typical SARs in world.

commercial SAR satellite in Canada after RadarSat-1. It inherits all working modes of RadarSat-1 and adds multi-polarization imaging and 3 m resolution imaging to the original one. JERS-1 [54] satellite was launched at Tanegashima Space Center in 1992 and is mainly used for geological research, agricultural and forestry applications, marine observation, geographic mapping, environmental disaster monitoring, etc. The satellite carries active SAR with fixed incident angle and single polarization (HH), works in L-band (center frequency 1.275 GHz), and has a resolution of 18 m. ALOS [54] was sent into sun synchronic and regressive orbit in 2006. ALOS uses high resolution and microwave scanning, mainly for terrestrial mapping, regional observation, disaster monitoring, resource investigation, etc. The satellite carries a L-band SAR. The satellite has the characteristics of multiple incident angles, multi-polarization, multi-mode of operation, and multi-resolution, with the highest resolution of 7 m. OSMO-SkyMed [55] satellite is the second satellite of COSMO-SkyMed high-resolution radar satellite constellation jointly developed by the Italian Space Agency and the Italian Ministry of Defense. The COSMO-SkyMed satellite has a resolution of 1 m and a scanning bandwidth of 10 km and has the capability of terrain interferometry. The COSMO-SkyMed system is a dual-purpose Earth observation system serving civilian, public, military, and commercial purposes. TerraSAR-X [55] radar satellite is the first satellite in Germany, and it works in the X-band with a center frequency of 9.6 GHZ. TerraSAR-X can circle the Earth in an orbit 514 km high and collect radar data all-time using an APAA with a resolution of 1 m, independent of cloud cover. The HJ-1C [56] satellite is a radar imaging satellite in the constellation of small satellites for environment and disaster monitoring and forecasting. It was launched in 2008 and is the first S-band synthetic aperture radar (SAR) satellite in China with a mass of 890 kg. It will form the first stage satellite constellation with the launched HJ-1A and HJ-1B satellites. In 2016, Gaofen-3 was successfully launched with the Long March 4C carrier rocket at the Taiyuan Satellite Launch Center. Gaofen-3 is a remote sensing satellite of China's high-resolution special project, a 1 m resolution radar remote sensing satellite, and the first C-band multi-polarization SAR imaging satellite in China with a resolution of 1 m. With 12 modes of working, Gaofen-3 is the world's most diverse SAR satellite. It can not only conduct a large-scale scanning but also conduct an accurate observation of a particular target and measure them accurately. It has all-weather, all-time, and all-round working ability. In 2020, China launched Haisi-1, the first internationally leading remote sensing satellite, with a C-band APAA, weighing less than 185 kg, with 1 m resolution, which can penetrate the cloud and acquire all-time, all-weather, and two-dimensional high-resolution radar data, regardless of time and adverse conditions.

2.6. Comparison of Main Characteristics of APAA on Different Platforms. The main characteristics of APAA on each platform are summarized in Figure 6.

The main characteristics of APAA on each platform have been compared and analysed in this section. GBR is a long-range target search radar. Ultra-high transmission power

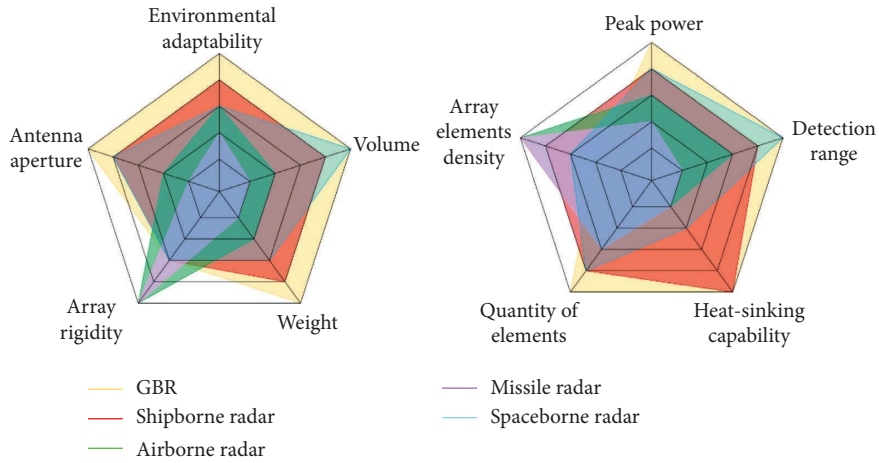

Figure 6: Characteristics of APAAs for each platform.

over several MW and large aperture electric scanning antenna arrays are generally used, and the working distance can reach several thousand kilometers. This type of radar is usually attached to tall buildings with a large number of elements and strong front stiffness. Also, it has a special-purpose temperature control system, is less tendency of deformation by load, and has the strongest environmental adaptability and stable detection performance. But its structure is cumbersome and its weight can reach over 1000 tons, and its detection power is affected by seismic load, ice and snow load, and non-uniform solar radiation. The vehicle-mounted subgrade APAR is another common form of radar, with long detection distance, lightweight, and strong maneuverability, which is mainly used for remote warning and recognition of stealth targets. The biggest problem it faces is the insufficient rigidity of the array structure due to its lightweight design. It is often deployed along the coast or in the Gobi region with a maximum wind speed of 30 m/s. Strong and time-varying wind loads can cause large deformations of the array structure, which severely restricts its detection performance.

Shipboard APAA has a smaller antenna size than GBR. It is installed on the "ship island" of the warship. Generally, it consists of four fixed arrays, each of which scans 90°. The radar has strong performance and can track dozens of targets at the same time for a maximum detection distance of several hundred kilometers, thus effectively intercepting high-altitude targets. It has more antenna elements and tighter arrangement than subgrade APAR, with strong rigidity of array structure. It has more antenna elements and tighter arrangement than subgrade APAR, but with strong rigidity of array structure, equipped with a better liquid-cooled heat dissipation device and a protective cover, which has strong environmental adaptability. It faces the problems of moisture-proof, mold-proof, and salt-mist-proof.

Airborne APAA is the most comprehensive radar in the world, with a detection distance of several hundred kilometers, multi-target tracking, and high resolution. The main loads it faces are high thermal power and random vibration. Because of the aerodynamic requirements of the fighter, the size of the airborne radar is limited by the size of the nose cone at the front. High power, large quantity, and tightly arranged T/R modules will generate a lot of thermal energy. Due to the lightweight design requirements, the heat dissipation capacity of the radar is limited. High temperature will cause slight distortion of the antenna array and degrade the performance of electronic components and ultimately affect the detection performance of the radar. At the same time, random vibration will lead to gain loss and pointing error of radar antenna when affected by factors such as aircraft engine and air convection, which will reduce the ability of radar to track targets.

The volume and quality of missile-borne APAA are limited by the aerodynamic requirements of the missile, the antenna diameter is small, the number of T/R components is large and arranged closely, and the heat dissipation capacity is insufficient. High-temperature ablation is the main reason that restricts the radiation performance of APAA on missiles. During the high-speed flight, the air around the antenna is intensely compressed by the bow shock wave. This causes strong friction with the surface of the radome and makes the surface temperature of the radome rise sharply to several thousand degrees Celsius. The ultra-high temperature will result in severe changes in material properties and thickness of the cover. Due to thermal radiation and heat conduction, the high temperature on the surface of the radome conducts to the interior and the antenna itself generates continuously a lot of heat, which eventually leads to distortion of the antenna structure. In this case, the radiation performance of the antenna will be seriously degraded, resulting in a significant decrease in guidance accuracy.

In order to reduce the weight of satellite, spaceborne APAA generally adopts lightweight design. With large radar antenna array area and insufficient structural rigidity, it is susceptible to the influence of complex thermal environment in space. The spaceborne APAA is mainly affected by the complex thermal environment in space. When entering and leaving the shaded area of the Earth, there will be a large temperature gradient on the antenna array, which will cause thermal dither of the structure of the antenna and thus severe dynamic structural deformation. Meanwhile, the

radiation performance of the spaceborne APAA will be reduced, resulting in a serious impact on the resolution and imaging accuracy of the APAA.

2.7. Structural-Electromagnetic-Thermal Theory of APAA. As a highly integrated electronic equipment, APAA has a complex mechanical structure and feeder network, and there are many errors sources in structure, heat, electromagnetic, and other aspects. Before discussing the connotation of SET coupling of APAA, this survey classifies various errors into two types. ① Feed errors and structural errors can be classified according to the source of the errors. Feed errors include radiation element failure, excitation current amplitude and phase error, device performance temperature drift, radiation element coupling, and digital phase shifter phase quantization error. Structural errors include two aspects: the errors in the manufacture and installation process of the antenna, and the structural distortion caused by the environmental load and temperature distribution in the antenna service. Note that in practical applications, structural errors may also cause feeding errors, such as changes in feeder impedance and inconsistent polarization direction. ② The errors can also be divided into random errors and system errors. Random errors cannot be predicted in advance, such as the amplitude and phase random errors of the exciting current, the failure rate of antenna elements, the errors caused by antenna fabrication, and the position errors in the installation of elements. By contrast, system errors can be predicted in advance and strictly controlled, such as radiation element coupling, digital phase shifter phase quantization error, and antenna array structure distortion under load. The error classification is presented in Table 5.

2.8. Effect of Antenna Array Structure Error. In APAA service, the environmental load and the temperature distribution of the antenna will lead to the distortion of the antenna surface. Also, random errors will occur during the manufacture and assembly of the antenna, which will affect the position of the antenna elements, generate a new phase difference distribution on the antenna aperture surface, and even cause the maximum radiation direction of the elements (e.g., the oscillator unit and printed dipole) to be offset with the distortion of the reflector plate. In this case, there is no longer a regular parallel arrangement, resulting in the mutual coupling of the elements and changes in the pattern. These factors will directly affect the antenna's electrical performance. Therefore, it is necessary to establish SET coupling to quickly determine the impact of antenna performance to support subsequent performance compensation, as shown in Figure 7.

The influence of antenna array structure errors on APAA can be divided into three categories: antenna array position offset, mutual coupling effect of antenna elements, and local deformation of antenna elements.

(1) Analysis of the position offset of the array antenna on the electric performance: Arnold et al. [57] analysed the effect of the structure bending deformation caused by airflow load on the detection performance of the array antenna mounted on the wing during flight. Takahshi et al. [58] pointed out that temperature changes in the space environment will cause thermal distortion of the spaceborne phased array antenna and seriously affect its radiation performance. The above studies show that service environmental loads can lead to antenna structure distortion and deteriorate antenna radiation performance, including gain, pointing accuracy, and sidelobe electrical equality. Besides, Wang [59] assumed two typical forms of deformation, i.e., bowl-shaped deformation and bending deformation, to investigate the influence of structural deformation on antenna radiation performance. The results show that the average side lobe level of −10 dBi can be obtained only when the structure error of the front is controlled within 1% of the wavelength range. Ossowska et al. [60] analysed the effects of random deformation, symmetric deformation, and asymmetric deformation on the radiation performance of the SAR antenna.

(2) Analysis of mutual coupling effect of antenna elements: The difference in the mutual coupling between APAA elements and the amplitude-phase error of the exciting current indicates that the mutual coupling effect cannot be reduced freely but can be compensated by some method. When the number of elements is reduced or the required side lobe level is low, especially in the case of beam scanning, the mutual coupling greatly affects the array antenna and must be compensated. Alibakhshikenari et al. have done a tremendous amount of very creative work to solve the problem of mutual coupling, and the research results are very valuable [61–69]. They have done a whole range of interesting research on the SIW technology, the metamaterial photonic bandgap (MTM-PBG), and metasurface, which effectively reduce the mutual coupling between adjacent radiation elements. Meanwhile, they have also used the MTM electromagnetic bandgap (EMBG) structure, the metamaterial decoupling slab (MTM-DS), the electromagnetic-bandgap (EMBG) structure, and a novel 2D metasurface wall to increase the isolation between radiation elements. Althuwayb proposed a simple method based on the metasurface concept to suppress the mutual coupling between the radiation parts of array antenna [70]. These works not only have very good research significance but also have very high engineering application value. Ossowska et al. [60] considered that only the spatial phase differences between the units need to be considered when estimating the electrical performance of the distorted array antenna and took the linear array antenna with $\lambda = 3.11$ mm, element spacing of 16.7 mm, and element number of 60 as an example to analyse the effects of symmetrical,

Table 5: Error classification of APAA.

Error sources	Error type	
	Random error	Systematic error
Structural error	Antenna manufacturing, installation errors	Load distortion (self-weight, wind, vibration, heat, etc.)
Feed error	Amplitude and phase error of excitation current, failure of radiation elements	Radiation element coupling, T/R module performance temperature drift, digital phase shifter phase quantization error

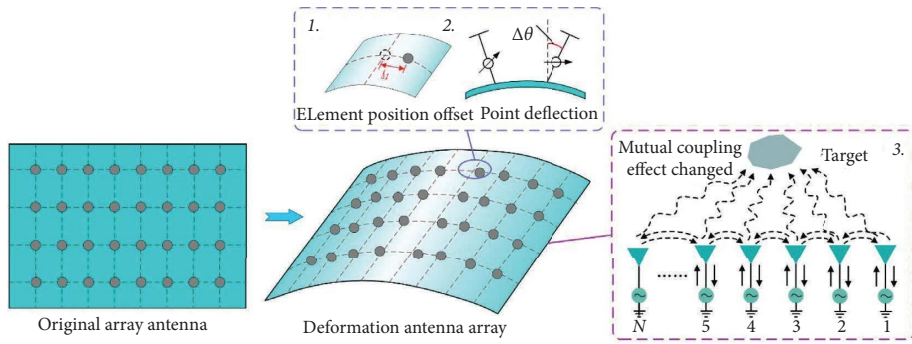

Figure 7: Structural-electromagnetic-thermal coupling relationship of APAA.

unsymmetrical, and random mechanical distortion on the radiation performance of the SAR antenna. The simulation results show that the gain of antenna decreases gradually with increasing deformation from 0 to 10 mm under symmetrical deformation, up to 1.73 dB, the 3 dB beam width of the antenna increases gradually, up to 0.21°, and the PSLR decreases gradually, up to 6.52 dB, without affecting the position of the main lobe. The asymmetric bending of the array plane has little influence on the antenna gain and 3 dB beam width, but the side lobes are asymmetric in that one side enlarges and the other side decreases. Farahani et al. [71] used a microstrip technology to construct electromagnetic bandgap (EBG) structures to mitigate the mutual coupling problem. A novel uniplanar compact electromagnetic bandgap (UC-EBG) structure is placed at the top of the antenna layer to reduce the mutual coupling between element separation and the patch antennas, to increase the increases antenna directivity. By adding two rows of UC-EBG to the designed antenna, 11 dB reduction in mutual coupling and 1.3 dB increase in directivity are achieved as compared to the array without EBG. The effect of the three rows of the UC-EBG superstrate on the mutual coupling has also been investigated. In this case, the mutual coupling is reduced about 14 dB compared to the array without EBG. Vendik et al. [72] used the impedance matrix Z to represent the mutual coupling relationship between antenna elements. The coupling current is expressed as the complex amplitude of the current distribution, the applied voltage, the impedance matrix, and the admittance. The coupling current distribution is calculated based on the complex amplitude of the current distribution, and the transfer coefficient and phase are calculated. The amplitude and phase of the exciting current are corrected by controlling the amplifiers/attenuators and phase shifters. Considering the mutual coupling of array elements, Zhang and Zhang deduced the relationship between the random error of amplitude and the phase of excitation current of the linear array and the average power direction diagram. Meanwhile, the influence of error on different array elements and different amplitude weightings was analysed [73].

(3) Analysis of the effect of local deformation of antenna element on electric performance: Deformation of the antenna structure will not only cause the position of the antenna element to offset, but also cause a significant change in the shape of the element, which will have a major impact on its performance. Mohammadi Shirkolaei et al. made an interesting research using the flexibility of microstrip antennas and designed an array antenna for medical purposes that can be mounted on the thighs, lumbar, or head of a human body [74]. First, a high gain stacked circular microstrip patch antenna with 2.45 GHz frequency is designed according to the maximum-gain theorem, and then a 1×4 array antenna is designed for mounting on the human thigh, and each antenna element covers 120°. This work is very important to promote the application of smart antenna in medical field. Bai et al. studied the influence of the bending deformation of the microstrip antenna in different directions on the radiation pattern [75]. Geng et al. took the microstrip antenna with defective ground structure as the research object and analysed the influence of the bending degree of the antenna element on the performance of the microstrip antenna. The result shows that the deformed antenna can work normally at each frequency band by changing the structure parameters, which provides ideas for the multi-band design of the microstrip antenna [76]. Wu and Ehrenberg studied the non-planar microstrip array antenna and pointed out that the design of the non-planar structure significantly affects the electric performance of the microstrip antenna, but the electric performance of the antenna can be improved by adjusting the excitation amplitude and phase [77]. Han studied the bending deformation of microstrip element of spaceborne array antenna under environmental load and proposed the equivalent size model to mathematically characterize the deformation element. The simulation experiments verified that the method achieves a good accuracy under certain deformation degrees [78].

The Key Laboratory of Electronic Equipment Structural Design of the Ministry of Education has been studying the coupling effect between antenna structure displacement field, temperature field, and electromagnetic field since the 1990s. The influence of structural deformation caused by mechanical vibration, wind load, and solar radiation on antenna electrical performance has been analysed. Kang focused on APAA. The SET coupling of the antenna is studied in-depth, and a structural-electromagnetic-thermal three-field coupling model is established, which can be used to quantitatively analyse the influence of structure deformation and temperature change on the electric performance of APAA [79–81].

2.9. Influence of Radome Structure and Physical Property Parameters. The radome is located at the front end of the APAA in missile, which is the main structural component of the APAA and a fundamental part of the radar guidance system. It ensures reliable operations of the APAA in supersonic and hypersonic flight. To achieve accurate guidance, the high electric performance of the APAA is demanded [16]. However, during high-speed flight, due to friction blockage, the aerodynamic heating between the surface of the radome and the airflow causes a dramatic increase in the surface temperature of the cover. This results in a huge temperature difference on the surface of the cover and the normal thickness, which ultimately leads to high-temperature ablation of the radome. This phenomenon becomes even more serious with the increase of flight speed, as shown in Figure 8.

The effects of high-temperature ablation on the antenna in a missile mainly include the following. ① Material parameters of the radome at high temperatures change, such as relative dielectric constant and loss angle tangent. ② High temperature causes ablation of radome surface, which changes the cover thickness. ③ The high temperature of the antenna radome will increase the antenna temperature in the radome through radiation and transmission, which will cause feed errors of the elements and finally deteriorate the electric performance of the ballistic antenna. Under the influence of high-temperature ablation, the material parameters and radome thickness will change. Qin and He [82] proposed that the ablation layer produced by the radome in high-speed flight would seriously affect the antenna electrical performance. However, the study only assumed that the ablation layer has fixed thickness and material parameters, and the surface morphology of the radome under actual ablation was not analysed. Weckesser [83] studied the material parameter changes caused by the surface temperature changes of an aircraft radome at a certain time during the automatic searching phase and its influence on the radome pointing error during scanning. Taking the radome cover as an example and based on the change of material parameters of the normal temperature gradient between 25°C and 1200°C, Parul and Jha [84] studied the changes of the phase shift, transmission coefficient, and reflection coefficient of the radome insertion using the non-uniform plane layer model. Based on the test data of the physical parameters of the antenna cover changing with temperature, Nair and Jha [85] analysed the variation of the transmission coefficient, pointing error, and cross-polarization level of the antenna cover during the scanning process. When considering both the temperature change and the ablation effect of the radome, only the radiation performance change of the radome under the influence of fixed ablation thickness and material parameters was studied.

2.10. Effect of Element Feed Error

2.10.1. T/R Module Performance Temperature Drift. The more T/R modules and the higher the frequency of APAA, the tighter the arrangement of components and the higher the thermal power density of the entire antenna array. The high temperature will change the amplitude and phase of excitation current and then affect the antenna's electrical performance. At present, the influence of temperature change on the feed current of the T/R module is mainly studied from two aspects: a thermal-electromagnetic analysis based on the circuit model and an experimental test. Zhong et al. [86] studied the influence of temperature on the T/R module of radar, established a simplified circuit model of the T/R module, and investigated the change of circuit performance with temperature. Yang [87] established the circuit model of the S-band phase shifter and simulated and analysed the amplitude and phase change of the exciting current output by the circuit model at different temperatures. The above studies provide a theoretical basis for studying the effect of heat on the performance of T/R modules. However, the internal circuits of the T/R modules are complex and interconnected, and further research is required to obtain accurate temperature effects. The magnitude and phase errors of the excitation current output by the T/R module under temperature influence are investigated by experimental test and engineering experience [81]. It is also a common method at present. Mohammadi Shirkolaei and Ghalibafan made a series of beneficial explorations on the components in the fuzzy array radar. They made great contribution to the future development of APAA by using novel component structures to improve the antenna performance. They proposed a novel magnetically scannable LWA based on the slotted ferrite-filled rectangular waveguide, which utilizes the balanced CRLH response of the proposed structure, achieves the continuous beam scanning from negative to positive angles, and enhances the gain of LW antenna through the position and number of slots on the broad wall of waveguide [88]. A novel leaky wave antenna is presented based on the substrate integrated waveguide structure. Through the combination of rectangular and H-shaped slots at the top of the antenna, the leaky wave antenna is capable of scanning the beam continuously from 2.3 to 87° by sweeping the frequency from 10 to 12.2 GHz [89]. It is meaningful to simulate uniaxial anisotropy by stacking three different layers of uniaxial anisotropic media, which enhance the bandwidth and gain while reducing the size of the antenna structure. A multi-

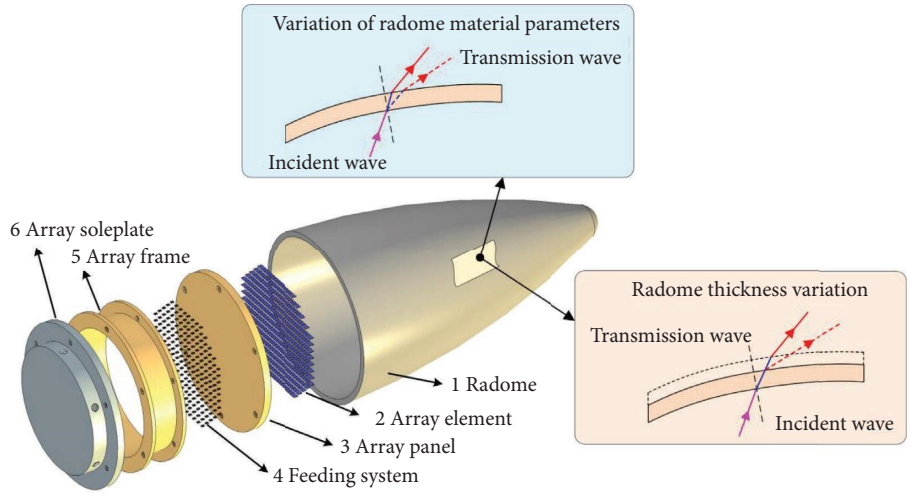

Figure 8: Schematic diagram of influence of material parameters and thickness changes of radome [16].

stack anisotropic cylindrical dielectric resonator antenna with high gain and wide bandwidth is reported [90]. This antenna is designed with three different stacks, and each stack consists of a multi-layer dielectric structure, which is the main reason for the wide bandwidth and high gain. The research results are very meaningful. A very interesting compensation matching method is also proposed for the design of the stable low-noise broadband microwave amplifier [91]. A hybrid optimization algorithm based on the combination of the genetic algorithm and conjugate gradients method is used to obtain low-noise figure, gain flatness, stability, and loss factor correlated with each reactive element and matching network accomplishment included together. An 8~16 GHz broadband microwave amplifier is designed to verify its application [92]. In order to solve the matching problem of the directional coupler, a very good method for mode matching of directional coupler in mode analysis is proposed and verified on directional coupler of X-band rectangular waveguide ports. The S-parameters obtained by this method can be used as the element value for calculating the equivalent circuit model. A very innovative W-band monopulse antenna planar waveguide combination network method is proposed [93]. The design consists of directional coupler, phase shifter, and H-plane bend. The design has many advantages such as compact structure, light weight, and low height, and it can be specially used for airborne applications and has a very good application prospect.

2.10.2. Array Antenna Power Ripple. Array antenna power ripple refers to the AC component superimposed on the output DC voltage. The antenna array power ripple factor refers to the ratio of the peak value of output ripple voltage to output DC voltage. It is a key indicator to measure the performance of the antenna array power supply. When the antenna array power supply supplies power to the T/R module, the AC component is superimposed on the output DC voltage of the power supply, i.e., the array antenna power ripple will produce amplitude and phase modulation to the exciting current in the T/R module, thus resulting in amplitude and phase error of the current [94]. As the temperature of the array antenna increases, the thermal drift of the electronic devices inside the front power supply changes the power ripple, which further changes the excitation current output by the T/R components. Wong and Ricciardi [95] studied the influence of different levels of biased power supply ripple voltage on the output spectrum of the high-power amplifiers in radar. Abe et al. [96] analysed the influence of power ripple on the output phase of multi-beam klystron in high-power applications. Yang [97] studied the influence mechanism of power ripple on the noise performance of low-noise amplifiers based on the principle of statistics. Wei [98] investigated the influence of amplitude and phase distortion of RF amplifiers caused by high-voltage power supply ripple on the quality of MTI radar transmitters. Zhang [99] analysed the influence of power ripple on the output performance of TWT amplifier. Tan et al. [100] studied the influence of power ripple on the performance of linear frequency modulation pulse radar and suggested that the power ripple supplied by the transmitter amplification link will lead to the amplitude and phase distortion of the signal.

2.10.3. Phase Shifter Quantification Error. Due to its simple structure and stable phase shift value, the digital phase shifter is commonly used in the T/R module of APAA. However, the phase-shifting values of digital phase shifters are not continuous and can only be shifted by an integer multiple of a minimum phase, so the phase obtained by the antenna is called quantization. In this case, a new class of problems arises in APAA, especially in low or ultra-low side lobe APAA. The phase quantification error of the digital phase shifter causes a series of parasitic side lobes in the antenna lobes, which ultimately raises the side lobe level of the whole antenna [101]. For example, Gao [102] used the probability and statistics method to obtain an estimate formula between the phase quantification error of the digital phase shifter and the lifting amount of the maximum

antenna side lobe level. In their study, the lifting amount of the maximum side lobe level was expressed as a function of the aperture efficiency of the antenna, the number of radiation elements, the side lobe level, and the number of digital phase shifters. The rounding method and carry method are often used to reduce the influence of phase quantization error in engineering applications. Liu et al. studied the suppression of phase quantization error by the random feed method [103]. Yang used the Monte Carlo method to solve the non-linear equations, analysed the errors of each phase shifter under a certain offset of the antenna beam, and calculated the angle offset probability of the antenna pattern under the normal distribution of the phase shifter error [104].

2.11. Structural-Electromagnetic-Thermal Coupling Model. During APAA service, environmental loads can lead to deformation of the array structure, deflection of the elements, and displacement of the position. Meanwhile, the temperature will also degrade device performance in the antenna and reduce antenna electrical performance. Conversely, a higher antenna performance imposes a more stringent requirement on structure and heat dissipation. Therefore, in APAA, there are interactions between the antenna structure, thermal performance, and electrical performance. The key to investigating the SET coupling of APAA is to find the mathematical relationship among the structure, thermal, and electromagnetic interaction and to establish the coupling model. Figure 9 shows the schematic diagram of the SET coupling of the APAA in a missile.

2.11.1. Establishment of the Structural-Electromagnetic-Thermal Coupling Model. In view of the mutual influence and restriction among the structure, heat, and electromagnetism in APAA, Kang of the Key Laboratory of Electronic Equipment Structural Design of Ministry of Education of Xidian University studied and established the SET coupling model of a rectangular grid, triangular grid, radome-enclosed antenna, and radar detection [79–81]. The important factors were considered, such as element position error, direction deflection, element mutual coupling, and device performance temperature drift, which makes an outstanding contribution to the SET coupling research of APAA. The influence of high-temperature ablation on antenna cover and antenna performance is analysed below, and the SET coupling model of APAA in the missile is established [16].

$$\begin{aligned} E_s(\theta,\phi) = {} & \sum_{n=1}^{N} f_n(\theta,\phi)\left[A_n + \Delta A_{nt}(T) + \Delta A_{np}(T)\right] e^{j\left[\varphi_n + \Delta\varphi_{nt}(T) + \Delta\varphi_{np}(T)\right]} \cdot \\ & e^{jk\vec{r}_n \cdot \hat{r}_0}\left[T_H'^2 \cos^4\phi_M + T_V'^2 \sin^4\phi_M + 2T_H' T_V' \cos^2\phi_M \cdot \right. \\ & \left. \sin^2\phi_M \cos\delta\right]^{1/2} \cdot \exp\left[-j(\eta_H' - \varphi_M')\right], \end{aligned} \tag{1}$$

where $f_n(\theta,\phi)$ is the directional pattern of the antenna element, $I_n = A_n e^{j\varphi_n}$ is the exciting current of the antenna element, and A_n and φ_n are their amplitudes and phases, respectively. Among them, the feed amplitude and phase errors caused by temperature drift of electronic device performance in T/R module are $\Delta A_{nt}(T)$ and $\Delta\varphi_{nt}(T)$, respectively. Amplitude and phase errors due to waveguide corrugated by array power supply are $\Delta A_{np}(T)$ and $\Delta\varphi_{np}(T)$, respectively. T_H' and T_V' are the magnitudes of the transmission coefficients of the horizontal and vertical polarized fields of the incident electromagnetic waves affected by high-temperature ablation, respectively. ϕ_M is the polarization angle of the electromagnetic wave. $\varphi_M' = \arctan\left[T_V' \sin^2\beta \sin\delta_i / (T_H' \cos^2\beta + T_V' \sin^2\beta \cos\delta_i)\right]$, $\delta_i = \eta_H' - \eta_V' \eta_H'$, is the insertion phase shift of the horizontally polarized field and η_V' is the insertion phase value of the vertically planned length.

2.11.2. Radar Detection Model. The concept of radar communication was introduced at the beginning of the 21st century [105]. Hall studied the influence of loss factor on radar detection performance and investigated in-depth the relationship between radar false alarm probability, pulse accumulation, and radar detection performance. Blake [106] studied the estimation of the radar range equation that summarizes the advantages of the previous radar equation, introduces many external factors (e.g., noise temperature and multi-path interference), and gives a more accurate radar distance equation. Skolnik [107] improved the radar detection distance equation and mainly discussed the influence of radar environment factors on radar detection distance. Brenna and Reed [108] analysed the method for estimating radar detection accuracy and proposed a good method for signal samples. Glass [109] derived the quantitative relationship between antenna amplitude and phase errors and radar beam pointing accuracy. Hsiao [110] investigated the effect of beam direction and 3 dB lobe width on radar detection performance and pointed out that low side lobes have better tolerance.

Taking the airborne APAA as an example, the detection performance of airborne radar is mainly affected by the maximum detection distance of the radar, the radar resolution characteristics, and the detection accuracy of the

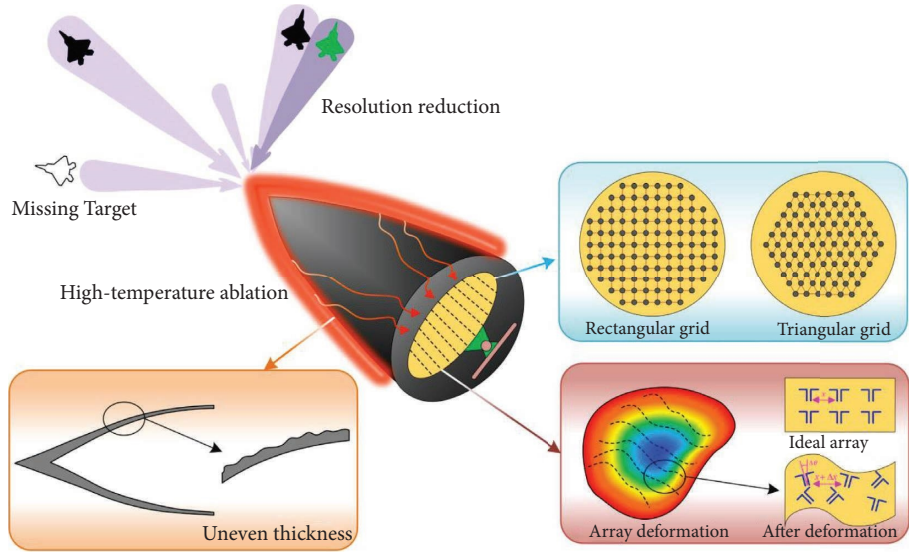

Figure 9: Structural-electromagnetic-thermal coupling of the APAA in missile.

radar. Xiu established the relationship between the electrical performance of the array antenna and the main detection performance of the radar [111]. The position error of array antenna elements can be used to quickly predict the detection performance of the radar. Specifically, the following three aspects are mainly studied: ① the coupling model between the longest detection distance of radar and antenna structure deformation; ② the coupling model of radar range resolution variation rate and radar speed resolution with antenna array deformation; and ③ the SET coupling model of radar ranging accuracy and radar angle measurement accuracy and antenna array structure deformation.

2.11.3. Scattering-Oriented Structural-Electromagnetic-Thermal Model. When the antenna structure is distorted due to the service environment, the position error of the antenna elements reduces the radiation performance of the antenna. Meanwhile, the phase distribution of the scattered waves is reflected by the element changes in space, which affects the scattering performance of the antenna. Currently, the studies mainly focus on the analysis and synthesis of antenna radiation performance [112], but scattering performance is less studied. The scattering field of APAA can be divided into two types: structure mode and antenna mode. The vector superposition of these two types constitutes the radar cross section (RCS) of APAA. The analytical calculation of the antenna structure mode item, antenna mode item, and the phase difference between them is usually very complicated. Lu [113] studied the scattering field of array antenna by combining the moment method of RWG basis function with the integral equation of antenna electric field. To calculate the scattering performance of microstrip patch antenna with arbitrary shape, Yuan et al. [114] proposed a comprehensive method for precorrecting fast Fourier transform and discrete complex images. Tanaka et al. [115] analysed the scattering field of the tapered slot array antenna based on the moment method and compared it with the measured results. When neglecting the mutual coupling and edge effect of antenna elements, the scattering field of the array antenna can be expressed as the product of the antenna element factor and the array scattering factor [116]. The above work provides a basis for calculating and analysing antenna scattering fields. However, the variation of the antenna scattering field is not considered when there are structure errors in the antenna structure. Wang established a coupling model between the structure and scattering matrix factor of APAA, studied the comprehensive influence of the position error of the antenna element on gain and RCS, and applied the particle swarm optimization (PSO) algorithm to optimize the installation height of all radiation elements on the array while guaranteeing the radiation performance of APAA. Based on this, RCS was effectively reduced [117].

3. Application of Structural-Electromagnetic-Thermal Technology in the Design and Manufacture of APAA

3.1. Environmental Load Impact Analysis. As shown in Figure 10, various environmental loads have different influence mechanisms on the electrical performance of APAA. Therefore, this section summarizes the influence of service environmental loads on the electrical performance of APAA on various carrier platforms, as shown in Table 6.

3.2. Analysis of Manufacturing Accuracy of Antenna Array. The manufacturing accuracy of the antenna significantly affects the radiation performance of the antenna. In recent years, many scholars have studied the coupling relationship between mechanism accuracy and antenna electrical performance. Su et al. [118] analysed the influence of structural accuracy on antenna polarization characteristics from two aspects: random errors and systematic errors. Hu et al. [119]

Figure 10: Service load of APAA on various platforms.

established the structure electromagnetic coupling model between the structural error of phased array antenna and the electrical performance and investigated the correlation between the antenna flatness, the installation accuracy of array elements, and the electrical performance of the antenna. Wang [59] analysed the influence of mechanical error and structural deformation on the performance of the planar antenna and studied the influence of two deformation modes on the normal and scanning sidelobe performance of phased array antenna in detail. Zaitsev and Hoffman [120] quantified the influence of Z-direction fluctuation on antenna beam pointing, sidelobe level, gain, and other performance indexes. Liu et al. [121] analysed the influence of each error influencing factor on the structural accuracy separately in combination with the array surface accuracy, antenna base shafting accuracy, array position accuracy, and calibration accuracy associated with telecommunication height in the radar structure. Wang used structure-electromagnetic coupling model of rectangular grid array antenna to analyse the antenna electrical performance variation under the influence of random error of element location installation [81]. The variation curve of antenna gain loss with random error of element position is plotted. In addition, the decrease of antenna gain under the influence of random error of element installation position is given when the size of array is different, and the relationship between array size, random error, and gain loss is determined.

The following conclusions can be drawn from the analysis of Figures 11 and 12. ① When the random error of element installation position reaches 1/10 of wavelength, the gain of antenna decreases, and when the random error of element position reaches 1/25 of wavelength, the gain of antenna decreases by 0.397 dB. ② When the number of elements is relatively small, the relation curve of antenna gain with random error of element position fluctuates greatly. ③ The number of elements is greater than 900 (30×30), the gain loss curve tends to a straight line, which indicates that the larger the APAA has, the less sensitive it is to the random error of the same magnitude, and the larger the magnitude of the random error, the greater its influence on the gain.

Althuwayb has done some very meaningful work in the field of supermaterials and terahertz. A very interesting on-chip antenna is designed and manufactured based on the metamaterial concept [122], which includes compact dimensions, wide bandwidth over the terahertz domain, low profile, and cost effective and great photoelectrical properties. Based on the characteristics of MTM and SIW [123], a very innovative millimeter-wave slotted bowtie antenna is designed, and the effective aperture area of the antenna is enlarged by using artificial magnetic conductor (AMC), and a wide frequency bandwidth along with high radiation performances has been achieved without affecting the physical dimensions. Proposed a technique to enhance the radiation gain and efficiency of metamaterial (MTM) inspired planar antenna using substrate integrated waveguide (SIW) technology for sub-6 GHz wireless communication systems has great application value [124]. In the tolerance design of antenna array, it is common to establish the SET coupling model between manufacturing accuracy and electrical performance of antenna array based on the Monte Carlo method. Mobrem [125] evaluated the profile accuracy error of planar antenna and peripheral truss mesh antenna based on the Monte Carlo method. Cui et al. [126] studied the effect of hinge repetition accuracy and profile machining accuracy of a reflector antenna on the overall profile accuracy error by using the Monte Carlo method. He et al. [127] put forward that considering together the waveguide size error, slot size error, and offset error when using the Monte Carlo method to analyse the relationship between radiation slot processing error and relative electrical performance of planar slot antenna can effectively improve the calculation speed of the moment method. Fan [128] applied the Latin hypercube experimental design method, genetic algorithm (GA), and Monte Carlo algorithm to systematically design the reflector structure of spaceborne antenna, thus obtaining the global optimal design result and improving the design efficiency. Alibakhshikenari et al. have done a lot of creative research in the terahertz field, and the research results are of great value. A very effective method to suppress the surface wave propagations and near field mutual coupling effects of the sub-THz array antenna using SIW technology is presented [129]. Substrate losses in millimeter-wave and terahertz circuits are suppressed, and antenna performance parameters such as impedance bandwidth, radiation gain, and efficiency are improved by using metamaterial and substrate-integrated waveguide (SIW) techniques, and the research result is innovative [130]. An interesting high-gain on-chip antenna on silicon technology antenna has been designed [131]. A metasurface on-chip antenna is constructed on an electrically thin high-permittivity gallium arsenide (GaAs) substrate layer [132]. A new terahertz on-chip antenna using standard CMOS technology is presented [133]. The comprehensive optimization of the radiation and scattering performance of the array antenna can be realized by adjusting the antenna structure and the position of the array element. Zhang et al. [134] optimized the radiation and scattering characteristics of the array antenna by adjusting the array element spacing. The simulation results show that the peak sidelobe level of the radiation pattern is reduced, and the grid lobe of single station RCS is effectively suppressed. Wang et al. [135] combined the electric field integral equation and the

Table 6: Service environment loads of APAA on different carrier platforms.

Platforms	Service environment loads	
	Main environment loads	Other environment loads
Land-based platform	Solar irradiation (temperature gradient on the inside and outside), wind load	Snow, ice, and earthquake
Shipborne platform	Humidity, salt spray, mold	Jolt, solar radiation, wind load
Airborne platform	High thermal power consumption and vibration of array	Shock
Missile-borne platform	High-temperature ablation	Array thermal power consumption
Spaceborne platform	Temperature gradient in and out of shadow area and space thermal radiation	Array thermal power consumption

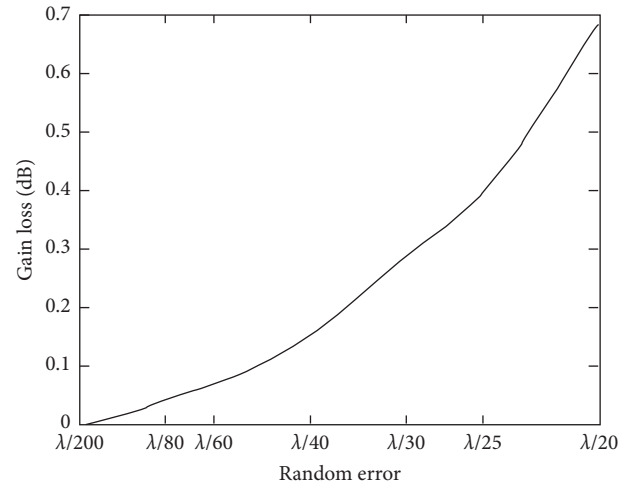

Figure 11: Gain loss versus random error of element position [79].

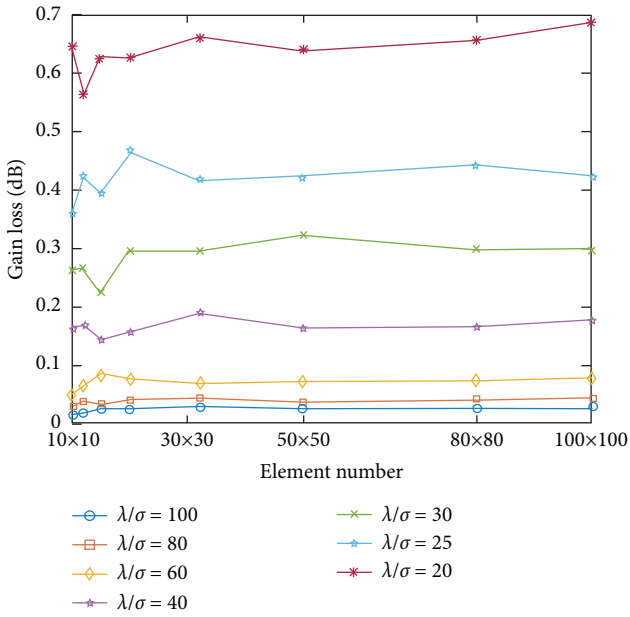

Figure 12: Gain loss in relation to array size and random error [79].

moment method of the RWG basis function to optimize the geometric parameters of the antenna, which not only improves the radiation performance of the array antenna but also reduces the RCS. Cong [136] staggered the anisotropic hypersurface elements around the traditional metal ground plate and adopted the mushroom structure as the antenna radiation aperture, which improves the antenna radiation performance and reduces the RCS in and out of the band. These are traditional optimization methods, and they can only reduce the RCS scattering peak. There are some problems, such as poor optimization effect of RCS main lobe and difficulty in mechanical structure design and manufacturing. Wang proposed a simple yet effective and fast comprehensive design method of APAA considering radiation and scattering performance [117]. The RCS structure and the electromagnetic coupling model of the APAA array were established, and the installation height of the radiation element was optimized and adjusted by PSO. The results show that the RCS of APAA can be greatly reduced while meeting the requirements of radiation performance.

3.3. Efficient Heat Dissipation Design. The development of heat dissipation technology is a three-generation process as shown in Figure 13. The first generation mainly uses air-conditioning cooling technology, but its thermal control ability is limited and the energy consumption is huge. The second generation uses high-efficiency thermal packaging/interface materials and microchannel technology to improve the heat transfer capacity of the cold plate and strengthen the "remote" heat dissipation capability. The third generation uses chip-embedded heat dissipation technology, which focuses on microflow control cooling technology inside and between high-power chips and introduces the cooling medium directly into the chip package to reduce the thermal resistance of the component. With a heat dissipation capacity of up to 1700 W/cm2, the current embedded heat dissipation technology has great development potential, and its research and application are expected to promote the innovation of antenna heat dissipation design.

At present, most of the radiation technology of APAA uses natural air cooling and forced liquid cooling. Natural air cooling has advantages of simple thermal control components, low cost, easy improvement, etc., but disadvantages of low radiation efficiency and low reliability. Forced liquid cooling has advantages of high heat dissipation efficiency, compact structure, etc., which is not complicated for thermal control components and does not have a high cost. In practical applications, it should be reasonably used in combination with conditions. As early as the late 1960s, the idea of cooling the design of antenna array amplifier components attracted much attention [137]. When the MEAR was designed in the USA, it was the first time in the world that a water-cooled method was used to heat the radar front, with a heat dissipation capacity of 64 kW/m^2 [138]. However, due to the limited process technology at that time, the water-cooling system could not be made compact, and it was not applied in airborne radar. In the 1980s, the United Kingdom adopted an efficient method combining closed-loop forced air cooling and forced liquid cooling to heat 128 groups of power amplifier components on the radar front on the SAMPSON MFR, which achieved a continuous and efficient heat dissipation capability [139]. Then, with the increase of phased array radar antenna elements, the radiation power and the heat generated by the front surface became larger and larger. Thermal pipe heat dissipation, thermoelectric refrigeration technology, jet impingement technology, and other technologies emerged. Loop heat pipes were used for heat dissipation on ETS satellites, achieving a design objective of maximum heat transfer capacity of 1000 W and a lifetime of more than 10 years [140]. The A-8 and A-11 series of missiles were adopted in Russian MiG fighters, in which the infrared detection system used thermoelectric refrigeration technology for temperature control [141].

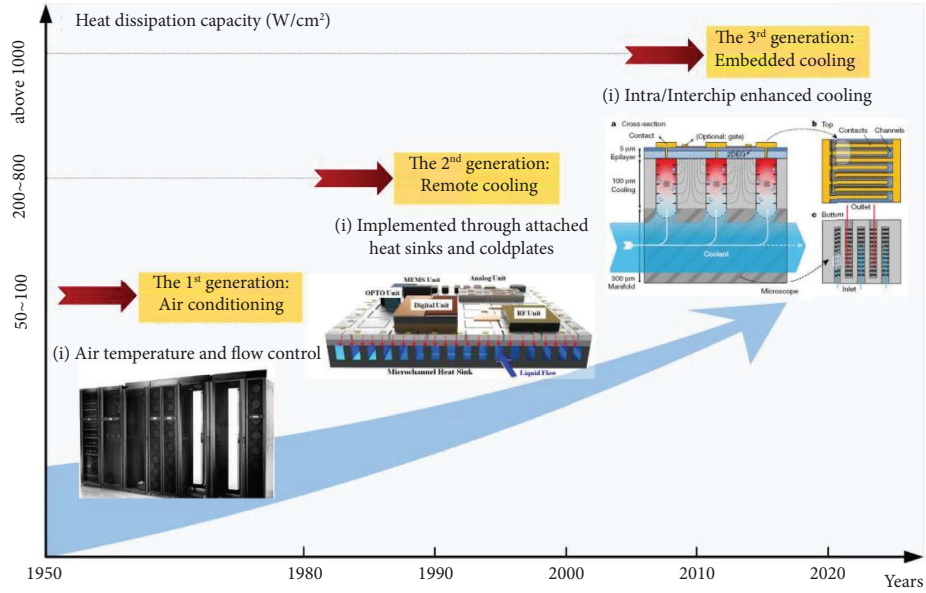

Figure 13: Development of heat dissipation technology.

With the development of antenna miniaturization and microfabrication technology, the microchannel cold plate provides a new solution to the thermal control of the phased array antenna. Because of the large heat dissipation surface area, the cooling effect of microchannels can be multiplied compared with that of traditional channels. Hui simulated the heat dissipation performance of the cold plate with a conventional flow channel and a microchannel structure. It was found that the heat dissipation capacity of the latter was nearly doubled, indicating that the microchannel cold plate has a good heat dissipation effect [142]. Wang et al. investigated the microchannel cooling technology of phased array antenna, summarized the influence of structure size parameters and thermal boundary conditions on the heat dissipation performance of the rectangular microchannel cold plate, and strengthened the heat dissipation by selecting reasonable boundary conditions and optimal channel size parameters [143]. Lu studied the heat flow characteristics of the phased array antenna microchannel from the perspective of equivalent modelling, which greatly improved the calculation efficiency of the thermal simulation [144]. These studies confirm the superiority of microchannel heat dissipation over traditional heat dissipation methods.

With the development of APAA towards higher heat flow density, the microchannel cold plate shows inadequate heat dissipation capacity and temperature uniformity. The emergence of embedded microchannel heat dissipation provides a solution to the heat dissipation of electrical appliances with a high heat flow density.

DARPA launched the ICECool program in 2012 to design cooling modules within/between chips to handle a heat flux of 1000 W/cm^2. Lockheed Martin demonstrated its ability to eliminate a chip-level flux of 1.1 kW/cm^2 and transistor-level heat flux of 30 kW/cm^2 and applied them to HEMT drains and gates [145]. In 2020, a monolithic integrated manifold microchannel cooling structure with higher efficiency than the currently available was demonstrated by co-designing microfluids and electronics in the same semiconductor substrate. Experiments show that a heat flux over 1700 W/cm^2 can be extracted with pumping power of 0.57 cm^2/W [146].

3.4. Lightweight Integrated Optimization. In the 21st century, spaceborne APAR based on the spaceborne platform has become an important means for military reconnaissance and strategic early warning. Considering the impact of satellite launch load and limited space environment, spaceborne APAR has more stringent requirements for improving resolution, working mode, and deployment orbit height, which makes it crucial to accurately control radar load weight. The lightweight spaceborne APAR mainly focuses on the lightweight of APAA, and its weight usually accounts for more than 80% of the load weight of the whole radar.

For the overall architecture optimization of spaceborne phased array antenna, the light low-profile scheme of single machine hierarchical layout combined with blind plug interconnection can be applied to replace the traditional single machine-independent design and cable connection, thus realizing the miniaturization of T/R components and further reducing the weight of power distribution network and cables [147]. Each type of single machine is designed as a chip structure, and the cable-free phased array antenna module design is realized to meet the requirements of lightweight antenna. Thin-film APAA is a phased array antenna integrated with a flexible thin-film antenna through a miniaturized T/R module. The antenna has many advantages, such as light weight, small folding volume, large aperture, and beam scanning. It can be used to meet the lightweight and deployable application requirements of spaceborne radar antennas in the future. Meanwhile, it is

considered by NASA, DARPA, and other departments as the core technical means to break through the bottleneck of the development of a large spaceborne antenna [148]. The antenna radiation array is made of thin-film material, and the expansion frame adopts an inflatable flexible or rigid-flexible combined support structure, which can effectively reduce the weight and folding volume of the antenna. It is expected to reduce the average weight of the antenna to less than $10\,kg/m^2$ [149]. Based on the new antenna architecture design scheme, the application requirements of the new design scheme can be met by equipment function integration and integrated design. The integrated feed network, T/R module, power supply, and wave control are designed to reduce the weight of the array. Also, the integrated design of power supply, wave control, and feed network in APAA adopts integrated circuit technology, which greatly improves the reliability of the array and reduces the weight and volume of the array. The new three-dimensional architecture chip of the T/R module uses integrated circuit technology to integrate many active devices on a substrate, thus eliminating the electrical connections between components. This can reduce loss and noise, improve reliability, and make the component structure more compact and lighter [150]. Compared with the current T/R module, the weight of this chip of the highly integrated T/R module can be reduced by more than 1/3. The adoption of the distributed power supply and beam control scheme is conducive to improving the reliability of the antenna and reducing the complexity of the design, which can further simplify the design and meet the design requirements of a lightweight antenna.

3.5. Sparse Array Design. The design method of the sparse array is to retain or remove the radiating elements at the position of the radiating elements of the full array. The excitation modes of the installation array element can be divided into uniform excitation and non-uniform excitation. Generally, uniform excitation is adopted in the design of a sparse array to simplify the feed network and the array elements. However, it is difficult to obtain an ultra-low sidelobe array because of uniform excitation. Therefore, in the design of ultra-low sidelobe array, non-uniform excitation is adopted, and the typical design includes Chebyshev array and Taylor array [151]. A sparse array has two main advantages. One is that, under the condition of the same array aperture, a sparse array needs fewer array elements, which can reduce the antenna cost and system complexity. The other advantage is that, with the same number of antennas, the array aperture of the sparse array is larger, which can improve the performance of DOA estimation [152]. The principle of sparse array design is to solve the array element position and the corresponding excitation of the sparse array according to the given periodic expected pattern and use the number of array elements as few as possible to approach the desired pattern [153].

At present, a variety of approaches have been taken to design sparse arrays. Brown [154] realized the sparse optimal array arrangement of the linear array on the premise of meeting the assumption of omnidirectional radiation element through the subaperture antenna division method. Yang et al. [155] used the least square method to fit the absolute phase characteristics of the main feature vectors of different Doppler channels to estimate the phase center, realizing array element position estimation of the wing conformal array. Meanwhile, GA and PSO are widely used in sparse array design [156]. Li et al. [157] transformed the sparse optimization problem of conformal array antenna into a linear regression problem of the sparse matrix. Based on the Euler rotation theorem, the guidance vector model of conformal array antenna was established. Taking the pattern of array element antenna on the same plane as the target of sparse learning, the sparse optimization model of conformal array antenna was established based on multi-task learning. Wang et al. established an electromechanical model of radiation and scattering performance of sparse array antenna to improve the stealth performance of the radar. With this model, they studied array element arrangement, position error analysis, realization of low side lobe, and tolerance design of sparse array antenna [117].

3.6. Performance Control Technology of APAA Structure in Service Environment. During the service process, APAA is affected by the external environmental load, resulting in different forms of local deformation and overall deformation of the antenna array, as illustrated in Figure 14. This degrades the electrical performance of the antenna, making it impossible to complete the detection task. Therefore, it is necessary to establish an array monitoring system to monitor the state of the antenna array in real time and make mechanical and electronic compensation to ensure that the antenna is in a high-performance working state.

3.7. Optimal Layout of Strain Sensors. APAA is developing towards multi-function, long life, large-scale, and high complexity. In complex service environments, the antenna is affected by environmental loads and faces the problems of structural function state change and damage accumulation, which will threaten service safety. Therefore, it is necessary to arrange multiple types of sensors in the antenna structure to monitor the health status of the antenna in real time. The layout of sensors directly affects the accuracy of antenna array information acquisition. Therefore, the optimal layout of sensors has always been a research hotspot in antenna structure monitoring. At present, the mainstream sensor layout methods are mainly divided into classical methods based on structural modal information, joint algorithms to overcome the shortcomings of single methods, intelligent layout optimization algorithms, and sensor methods considering uncertainty.

(1) The classical method [158]: The effective independence method is a reverse order deletion method, which is first applied to the on-orbit modal analysis of large spatial structures. The effective independence method was first proposed by Kammer. It is considered one of the most effective sensor

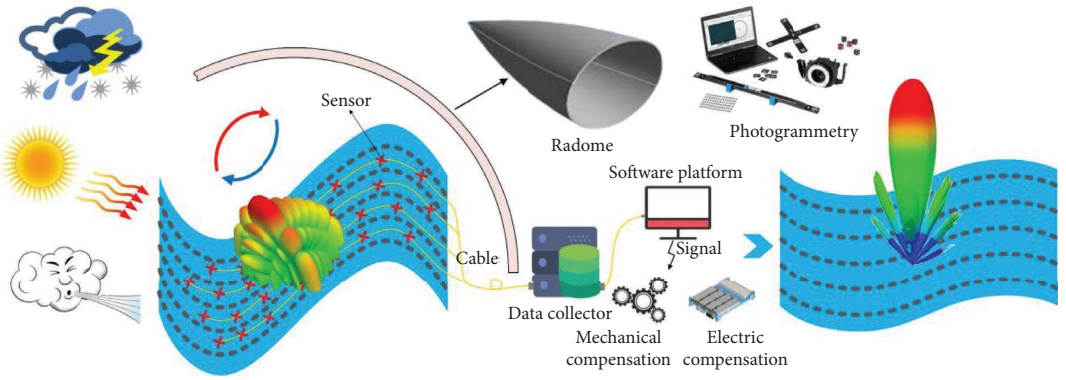

Figure 14: Schematic diagram of APAA array monitoring and performance regulation in service environment.

optimization methods, and it is also the most widely used and mature method. MinMAC is a typical positive order addition method. Its main idea is to match the structural modal shapes collected and identified by the actual dynamics with those calculated by the theoretical reference finite element method as much as possible. The modal matrix summation and quadrature method calculates the sum and product of the absolute values of each element in the modal matrix and takes the larger value of the row vector as the position of the sensor arrangement in decreasing order. The two methods are typical modal kinetic energy methods, and their biggest advantage is that they can effectively prevent the sensor from being arranged at the nodes of each modal mode of the structure and the degrees of freedom with a small modal kinetic energy. Besides, the origin residue method, QR decomposition method of modal matrix, SVD, and GRM and its improvement and equivalent method are also commonly used.

(2) The joint method [159]: An effective combination of various classical methods can better achieve the optimal layout of sensors. However, the measurement information is easy to be submerged in the noise because the effective independence method can only reflect the modal independent performance without considering the modal energy parameters in the structure. Therefore, in recent years, considering the shortcomings of this method, reverse order deletion methods have been proposed based on effective independent joint modal energy, such as four combination methods based on effective independent method and other four indicators, the combination algorithm based on energy coefficient and effective independent algorithm, the combination algorithm based on effective independent method and modal energy, the combination algorithm based on MAC, QR decomposition, and effective independence method, and other joint algorithms. The combination method for achieving sensor optimal layout considers the modal independence and anti-noise ability and improves the signal-to-noise ratio of sensor sampling to a great extent, thus achieving sensor optimal layout. However, these methods are only applicable to structural models with fewer degrees of freedom.

(3) The optimization method [160]: With the development of the intelligent optimization algorithm, the traditional iterative algorithm is not suitable for the problem of sensor optimal layout of large structures because it only depends on a certain order to screen one by one. Meanwhile, the optimization method develops further to the global optimization algorithm, which plays an important role in the optimal layout of sensors of large structures. Modern intelligent optimization algorithms represented by GA, PSO, MA, WA, K-means clustering optimization algorithm, etc. directly promote the application of sensor optimization layout to high-rise buildings, bridges, dams, large-span flexible structures, and other super-engineering projects with giant scale, ultra-large scale, and massive degrees of freedom. However, this does not mean that the classical sensor optimal placement theory has lost its position. When most intelligent optimization algorithms are adopted to solve the sensor optimal layout problem, the optimization objectives are usually derived from classical theory. For example, the determinant of Fisher information matrix and the root mean square error of non-diagonal elements of the MAC matrix are derived from the EFI and modal confidence criterion method.

(4) The sensor method: Due to the limitations of processing technology, instruments, equipment, and measurement technology, the uncertainty in the structure to be monitored and the uncertainty in the data acquisition process are difficult to avoid and cannot be eliminated. To reflect the influence of the two factors on the optimal placement of sensors, extensive research has been conducted on the optimal placement of sensors in the field of uncertainty such as sensitivity and robustness [161]. Castro-Triguero et al. [162] studied the optimal sensor layout scheme of the wooden structure by using the probability statistics method. Meanwhile, for the

uncertainty optimization of the sensor arrangement of the truss structure, it is pointed out that no matter the existence and size of the uncertainty parameters, there are always some deterministic sensor arrangement positions that will be retained under the uncertainty conditions. Based on the information entropy theory, Vincenzi and Simonini [163] achieved optimal or suboptimal arrangement results of sensors when structural uncertainty and noise coexist in structural health monitoring and modal testing. To overcome the lack of considering uncertainty in the effective independence method, Kim et al. [164] proposed a new random effective independence method by retaining the deterministic part and deducing the additional random term, which can better realize the linear independence of the modal matrix under the average effect. In addition, Papadimitriou and Lombaert [165] established an optimal layout method of sensors based on the error correlation prediction theory. Considering the difficulty of measuring the uncertainty in structural dynamic parameters, based on the advantage of the non-probabilistic method that only needs to obtain the boundary of uncertain parameters, Yang et al. [166] established the method for determining the number of sensors with interval uncertain parameters and analysed the layout possibility and the robust optimization mode. Also, the interval number relation and GA were used to analyse and optimize the discrete uncertainty problem, and the possibility of sensor layout and a more robust sensor layout scheme were obtained.

3.8. High-Precision Shape Reconstruction of Antenna Array. With the development of APAA, large aperture and high-frequency band have become the development trend of the APAA. As antenna aperture and frequency band increase, the requirements for antenna array accuracy are also improved. In the service process, the phased array radar is easy to be affected by the external environmental load. In this case, the structural deformation of the antenna array appears, and the phase error between antenna elements occurs, which causes a deviation from the design shape and seriously affects the electrical performance of phased array antenna. Therefore, it is necessary to accurately measure the position and attitude deviation of the phased array radar array and compensate for the electrical performance of the antenna [59].

In the field of antenna deformation reconstruction, the commonly used methods include the modal method, inverse finite element method, Ko displacement theory, and neural network method. Based on the strain displacement conversion relationship of the modal method, Zhou et al. [12] obtained the antenna variables through the strain data measured by the fiber Bragg grating sensor embedded in the skin antenna, established the electromagnetic strain coupling model of the antenna, compensated for the phase error caused by the deformation of the skin antenna, and verified the feasibility of the modal method. Yuan et al. [167] conducted simulation and experimental research on beams and wings with equal strength based on the Ko displacement theory, and the results confirmed the effectiveness of the method. Ko displacement theory is mainly based on the stress model of the Euler–Bernoulli beam. It is suitable for reconstructing a typical beam structure instead of objects with a complex structure. Alioli et al. [168] reconstructed the deformation field and pressure field of the membrane wing through the construction of the membrane element with the inverse finite element method and proved that the method has good real-time performance. The inverse finite element method does not need to analyse the material properties and the object modes in advance. It can solve the deformation field only by constructing the corresponding inverse element and combining the strain data. Also, it is easy to realize, but it is only suitable for typical beam structures and is greatly affected by the measurement error. Based on the combination of simulated annealing and neural network, Bruno et al. [169] constructed the relationship between strain and displacement of the target structure through training experimental samples and then inferred the deformation of the structure through a small amount of measured strain. The neural network method usually requires massive sample data of the target structure, which is greatly affected by the error of the sample data. Li [170] from Xidian University analysed the randomness of modelling noise and measurement noise and proposed an array shape reconstruction method based on the Kalman filter. According to the maximum likelihood criterion, the variance matrix of modelling and measurement noise was also included in the filtering iteration process to update the variance in real time and accurately reflect the characteristics of noise at this time, thus reducing the accumulation of errors in the iteration process and making it more suitable for engineering applications.

3.9. Compensation for Quantization Error of Digital Devices. To alleviate the deterioration of the electrical performance of the antenna under different working environments and ensure the performance of the antenna during operation, the antenna pattern can be corrected by inputting the corresponding compensation calculated with the digital attenuator and the digital phase shifter. Although having the advantages of simple structure, low energy consumption, fast operation speed, low control voltage, and easy computer control, attenuators and phase shifters are subject to their inherent quantization properties. They can only process discrete values and cannot realize continuous changes of amplitude and phase values according to the compensation obtained by the antenna electrical performance compensation method, which leads to the problem of amplitude and phase quantization and causes amplitude and phase quantization errors [171]. For example, the phase value of an m-bit phase shifter divides 360 degrees into 2 m nominal values. The minimum value is 0, and the maximum value is $360^{\circ}/2\,\mathrm{m}$. The phase value does not change continuously. In this case, the phase value of the phase shifter can only take the nominal value close to the required phase value, resulting in

phase quantization error [172]. On the one hand, the phase quantization error will broaden the main lobe beam, decrease the gain, and increase the SLL. On the other hand, it will deteriorate the beam pointing accuracy of the antenna and finally reduce the electrical performance of the antenna [173]. To achieve a better compensation effect of antenna electrical performance, considering the quantization error of the digital attenuator and phase shifter, a calculation method of phased array antenna compensation was proposed. Firstly, minimum attenuation and minimum phase shift are determined according to the step value and the number of bits of the attenuator and phase shifter. Then, based on the SET compensation model of the APAA, the amplitude and phase of the array element to compensate for the electrical performance of the deformed antenna are calculated. By comparing the amplitude and phase of the array element with the minimum attenuation and minimum phase shift, quantization amplitude compensation and quantization error compensation of the antenna element are determined to ensure the optimal electrical performance of the antenna. Based on the above calculation method of phased array antenna compensation, Zhou [174] developed the calculation software of electrical performance compensation of APAA considering the quantization error of digital devices. The software can quickly calculate the amplitude and phase compensation of the antenna, thus helping to reduce the influence of quantization error on the compensation effect and correct the compensation amount of APAA. The correction effect of quantization error can also be evaluated by comparing the two amplitude and phase compensation amounts before and after quantization error. Yang et al. [175] proposed to use the recursive comparison compensation phase feeding method instead of the traditional deterministic phase feeding method to reduce the influence of phase quantization error of phase shifter on phased array antenna beam pointing accuracy and antenna beam performance. It was proved that the recursive comparison compensation phase feeding method can reduce the influence of phase quantization error and alleviate the maximum and mean square deviation of antenna beam pointing error, thus improving the beam pointing accuracy of the phased array antenna.

4. Calculation of Excitation Current Compensation Based on Structural-Electromagnetic-Thermal Coupling

In Figure 15, two main electrical performance compensation methods of APAA are summarized: structural compensation method and electronic compensation method. The structural compensation method achieves compensation by controlling the deformation or adding an active adjustment device to the mechanical structure. The electronic compensation method achieves compensation by correcting the amplitude and phase of the excitation current of the antenna element.

The structural compensation methods of APAA can be divided into the following. ① Active adjustment of the array structure: An actuator or adjustment mechanism is adopted to control the structural accuracy of the antenna array and reduce the structural deformation. Hu [176] used the adjustment mechanism to adjust the subarray to improve the flatness of the array considering the decline of the array accuracy caused by the large weight of the phased array antenna. This method can actively compensate for the influence of structural errors, and it is applied to the performance compensation of phased array and reflector antenna. However, its implementation requires the structural adjustment device to be installed in the antenna system. ② Structure size control of active devices: In the APAA system, the structural size of the active device and the electrical performance of the antenna affect each other. The electrical performance of the antenna can be compensated by controlling the structural parameters of the active device. Son et al. [177] compensated for the influence of phase errors by adjusting the length of the phase shifter cable. This method is suitable for testing and calibrating the antenna in the manufacturing stage and compensating the phase errors of the antenna by adjusting the structure of the active device. However, it is not feasible in the service stage of the antenna. ③ Application of shape memory materials and self-calibration devices: This can automatically compensate for the electrical performance of the antenna. Song et al. [178] embedded a shape memory alloy wire in the honeycomb structure to compensate for the influence of thermal deformation of the antenna structure. This method can be applied to spaceborne APAA. To sum up, the structural compensation method can compensate for the influence of the structural deformation of the antenna. Especially for the phased array antenna with subarray, the structural accuracy of the array can be improved by adjusting the subarray structure. However, due to additional adjustment devices in the structural compensation method, the antenna system will have a large complexity.

The electronic compensation methods of APAA can be mainly divided into the following. ① Phase correction based on the "phase scanning" principle [179]: This type of method corrects the beam direction by controlling the phase difference between array elements to make it point to the target direction. For the foldable phased array antenna array [180], the maximum beam direction deviates from the target direction due to its own structural form. By controlling the feed phase of the array element, the direction can be adjusted back to the target direction to correct the beam direction error. However, this method has limited effect on SLL compensation. ② Optimization of the excitation current phase or amplitude phase: This type of method compensates for the comprehensive electrical performance of the antenna including pointing accuracy, gain, and SLL. Son et al. [181] used GA to optimize the phase of the excitation current of the array element to achieve the maximum received power of the antenna to compensate for the phase error of the antenna. However, the optimization method usually needs a large number of iterative processes, which is time-consuming and cannot realize fast real-time compensation. ③ Constructing the pattern correction coefficient, reconstructing the antenna pattern, and compensating for the influence of array element failure and mutual coupling

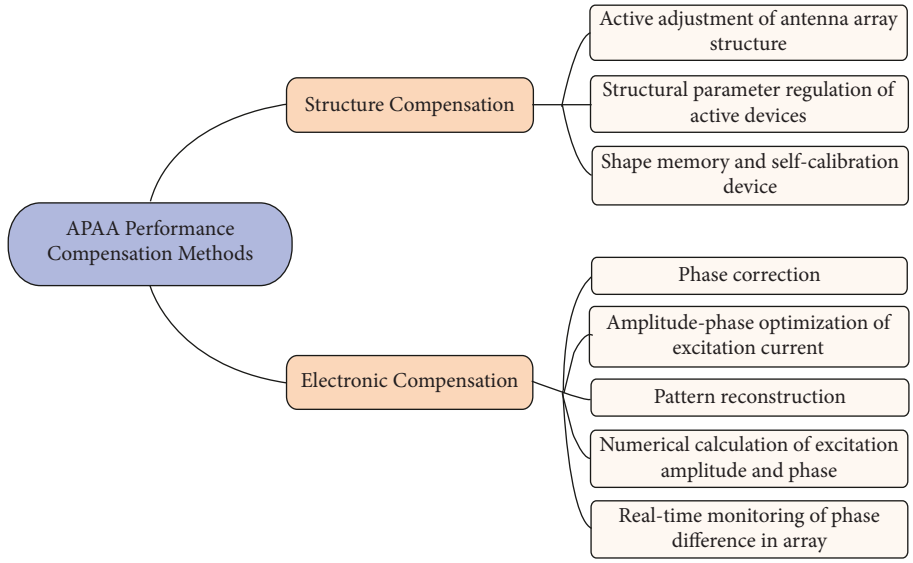

Figure 15: Compensation method of APAA.

between array elements on the electrical performance of array antenna: Steyskal and Mailloux [182] adjusted the weight coefficient of the non-failed array element and reconstructed the antenna pattern to reduce the influence of the failed array element when compensating for the failure of the array element. ④ Calculating the phase or amplitude phase compensation of the excitation current by combining with the numerical method: This method comprehensively considers the characteristics of the numerical calculation method and the requirements of antenna electrical performance and constructs the calculation model of excitation current phase or amplitude phase adjustment. Compared with the optimization method, it can quickly determine the compensation amount of excitation current [183]. ⑤ Monitoring the phase difference in the array in real time to compensate for the radiation performance of the antenna: Schippers et al. [184] installed analog integrated circuits on each array element to monitor the phase difference between the array elements in real time to regulate the phase of the array element and compensate for the influence on the radiation performance of the antenna. This method can only effectively compensate for the phase difference between antenna elements. Compared with the structural compensation method, the electronic compensation method can compensate for the influence of array element structural deformation and feed error on the antenna radiation performance without increasing the weight of the antenna structure, which provides a basis for real-time compensation of the antenna radiation performance.

Wang et al. of Xidian University proposed an amplitude and phase compensation method based on the SET coupling model and minimum square error and an amplitude and phase compensation method based on the SET coupling model and FFT for large-aperture ground-based APAA [9]. The two amplitude and phase compensation methods were compared with the phase compensation method. Considering the radiation performance and scattering performance of airborne APAA, a scattering performance evaluation model including the statistical characteristics of random structural error was established, which solves the problem that it is difficult to quantitatively evaluate the influence of structural error on antenna scattering performance. For the missile-borne APAA flying at supersonic and hypersonic speeds, two amplitude and phase compensation methods were proposed to effectively compensate the antenna gain, SLL, and beam direction under multiple frequency points and scanning angles. The space thermal environment leads to the thermal deformation of the array of spaceborne APAA. Besides, the strain electromagnetic coupling model of APAA was established, and phase and amplitude compensation methods based on the strain electromagnetic coupling model were proposed [81]. Finally, the array deformation and strain information measurement system was built, and the effectiveness of the strain electromagnetic coupling model and the compensation method was verified by experiments.

4.1. Compensation under the Influence of Radome. To reduce the influence of high-temperature ablation on the radiation performance of missile-borne APAA, Wang et al. took a hypersonic missile-borne APAA as the research object [16]. The radome heat flux under the influence of high-temperature ablation was obtained by aerodynamic thermal analysis, and the real-time temperature distribution and ablation morphology of radome were obtained by transient thermal analysis and adopting the "life and death unit" method. Meanwhile, the electrical properties of missile-borne APAA were analysed and compensated at multiple frequency points and scanning angles. The results show that high-temperature ablation at different scanning angles and frequencies will seriously reduce the electrical performance of missile-borne APAA, especially when the thickness of the cover in the scanning direction changes. When the working frequency of the antenna increases, the impact of high-temperature ablation on missile-borne APAA becomes

more serious. In addition, by adjusting the amplitude and phase of the excitation current of the antenna array element and compensating for the radiation performance of the antenna under high-temperature ablation, the main electrical parameters of the antenna such as gain, beam pointing accuracy, and SLL can be fully compensated, which effectively ensures the reliable working performance of the missile-borne APAA during flight. Two calculation methods of excitation amplitude and phase compensation are given below to achieve reliable radiation performance of missile-borne APAA at a single frequency point, single scanning angle, different scanning angles, and different frequency points.

(1) Amplitude and phase compensation based on the variation of radiation performance of a single array element of radome antenna: According to the SET model of the missile-borne antenna, the amplitude change rate and phase change amount of the electrical performance of the missile-borne antenna under the influence of high-temperature ablation can be obtained. By adjusting the amplitude and phase of the excitation current of the antenna array element, the amplitude change rate and phase change amount of the missile-borne antenna can be compensated for, so that the electrical performance of the compensated system is close to the ideal one.

(2) Amplitude and phase compensation based on the least square error of overall electrical performance of radome antenna: To compensate for the electrical performance of a missile-borne antenna in a certain scanning range or frequency band, a compensation method based on the least square error of the overall electrical performance of the radome antenna was proposed. Specifically, to reduce the influence of high-temperature ablation on the electrical performance of missile-borne APAA in a certain scanning range or scanning frequency band, the square error between the electrical performance of compensated APAA and the ideal electrical performance must be minimized.

4.2. Software Tool for Performance Compensation of APAA. The electronic devices in APAA have a high distribution density, and the complex mechanical structure of the antenna will produce structural deformation due to self-weight, vibration, and complex working environment. This results in problems such as antenna gain reduction, sidelobe increase, or beam pointing deviation. Therefore, it is necessary to determine whether the electrical performance of the antenna meets the design requirement in real time.

When traditional methods are adopted to evaluate the influence of structural errors on the electrical performance of the APAA, the simulation calculation of the APAA model must be carried out first. The existing general commercial electromagnetic simulation and analysis software (HFSS [184], CST [185], and ADS [186]) has a huge workload in the early modelling process and needs to apply complex loads and constraints and set boundary conditions. Also, the solution process consumes a long time, which cannot meet the demand of rapid prediction of antenna electrical performance [187–189]. Since the electrical performance of APAA will deteriorate under the influence of service environment load, it is necessary to adopt appropriate electrical compensation methods to improve the electrical performance of the antenna by compensating the amplitude and phase of the excitation current of the antenna element. So far, there is no mature commercial software to compensate for the electrical performance of the antenna under structural errors to offset the effects of antenna gain decline, sidelobe rise, and pointing deflection.

The research team of Xidian University designed and developed the electrical performance and compensation calculation software for deformed APAA, including the electrical performance calculation software, the compensation calculation software, and the compensation calculation considering quantization errors. Meanwhile, the team developed the integrated design software of the electrothermal machine for APAR, which can carry out mechanical and thermal simulation analysis of antenna structure and can quickly calculate and display the results. Software operation can reduce the workload of antenna designers, significantly improve their work efficiency, and provide a reference for scientific research and engineering applications [80, 174, 190]. Here are some key common technologies of software development:

(1) Numerical calculation software interface technology: the task of quickly calculating the electrical performance of APAA can be realized by using the engine function of the MATLAB engine to realize mixed programming of C++ Builder and MATLAB.

(2) CAX software interface technology: ① In the parameterization process of the APAA model, Pro/E secondary development technology needs to be used, and the basic seamless connection with Pro/E can be realized through the Pro/Toolkit development tool. ② As for mechanical simulation, ANSYS has powerful functions, a high utilization rate, and good openness. ANSYS is usually selected as the mechanical simulation analysis software in the mechanical analysis of antenna structure. Through the ANSYS batch file, the ANSYS software can automatically execute the APDL file, automatically analyse the antenna model, and display and extract the calculation results. ③ For thermal analysis, the software uses Flotherm to carry out a thermal simulation on the model, writes XML file in VBA language, starts Flotherm batch file, automatically opens Flotherm software, and uses Flotherm to call XML file to complete thermal analysis.

(3) Data processing technology: In the software development stage, database operations are involved. It is necessary to connect the software with the database and add, modify, or delete the data information in the database. C++ builder provides BDE (Borland

Database Engine), ADO (ActiveX Data Objects), and other database connection technologies. To operate the database more efficiently, ADO technology is selected as the connection mode between software and database.

4.3. Future Technology Trends. Terahertz APAA can detect smaller targets and achieve more accurate positioning than microwave antennas, and it has higher resolution and stronger anti-interference ability. It is an important development direction of high-precision detection and imaging in the future. Meanwhile, terahertz APAA has excellent ability to penetrate sandstorms and fog, and it can realize all-time and all-weather battlefield situation awareness. It has broad application prospects in military reconnaissance, military mapping, and space situation awareness [191, 192]. In recent years, the new generation of aircraft has put forward higher requirements for antenna intelligence and structure and function integration in airborne equipment. Thus, it is urgent to develop an antenna with high integration and excellent mechanical and magnetic performance. Currently, a skin antenna with conformal and load-carrying capability is mainly used. Compared with the traditional airborne antenna, the smart skin antenna technology reduces the weight and volume of the antenna and improves the aerodynamic performance, stealth performance, electronic countermeasure performance, and structure utilization ratio of the aircraft [193–195]. With the improvement of process level, the shape of millimeter-wave phased array antenna over 30 GHz will change a lot. That is, by using advanced heterogeneous packaging technology and microsystem integration technology, phased array antenna and even rear-end radio frequency and digital processing will appear as a complete SiP and SoC and may be reintegrated with other types of sensors such as sound, light, and magnetism sensors [196–198]. To meet the requirements of high frequency band, high integration, and high conformal load bearing of APAA in the future, the SET coupling technology will develop in the following aspects:

(1) Compensation for the electrical performance of APAA affected by uncertain parameters: APAA has a complex structure, harsh service environment, and time-varying characteristics. There are many uncertainties in the service environment, material mechanical properties, structural geometry, load bearing, etc. Moreover, important electronic components such as phase shifter and attenuator may cause performance degradation or failure due to the external load, and the uncertainty of electric compensation needs to be considered.

(2) Circuit model establishment and transmission performance prediction in the high-frequency domain: As microwave products develop towards broadband, miniaturization, and lightweight, the coupling effect of different transmission line conversion and interconnection processes on transmission performance becomes increasingly obvious in the high-frequency band. The electric length of the transmission line is close to the wavelength, and the parasitic effect of the shape of the interconnection point will seriously change the amplitude and phase of the signal, producing microwave effects of electromagnetic fields such as time delay, amplitude attenuation, signal reflection, and crosstalk when the signal is transmitted on the interconnection line. At present, the circuit equivalent model based on resistance, capacitance, and inductance suffers from some problems, such as inaccuracy. However, analysis based on finite element software is often time-consuming, and its performance analysis results are greatly affected by the accuracy of the model. Circuit analysis in the high-frequency field has always been a difficult problem in electronic manufacturing. Using the SET coupling model, the mapping relationship between the circuit structure and its electrical performance can be established, and the performance prediction accuracy and efficiency of the circuit model can be improved.

(3) Guarantee and maintenance of APAA throughout its life cycle: APAA has a complex structure, long service period, and bad working environment. It is crucial to realize failure prediction, fault diagnosis, and maintenance of complex electromechanical equipment and ensure efficient, reliable, and safe service of APAA. Based on the digital twin technology, the geometric model, finite element model, material property, acquisition data of various sensors, and production/inspection/maintenance data of APAA can be used to establish the digital twin model of APAA. This can comprehensively integrate the status monitoring, fault prediction, and maintenance decision of the phased array to improve the service life and reliability of the antenna. Based on the SET coupling theory, the model modification technology of electrical preparation, the sensor layout algorithm oriented to state detection and real-time regulation, and the control method of antenna performance are developed to improve the accuracy of the digital twin model and ensure the reliable service of APAA.

(4) The SET coupling model can also be developed and applied to other fields in the future, e.g., wind speed prediction. Wind load, as a common load, greatly affects large electronic equipment, such as large reflector antenna and large ground-based radar. Therefore, problems caused by wind must be solved. Meanwhile, as the integration of electronic equipment is becoming higher and higher, it brings significant challenges to heat dissipation performance. Based on the SET coupling model, the optimal heat dissipation scheme can be obtained by combining the structural characteristics of electronic equipment with its working performance, which will have a great application prospect in cost-saving and capacity improvement. In another field, new

Table 7: SET technology of APAA for service environment and its application.

Service loads of APAA	① Ground-based: array temperature gradient caused by solar irradiation, wind load, rain and snow, seismic load ② Shipborne: humidity, salt spray, mold, inertial load ③ Airborne: high thermal power consumption in array, vibration, impact ④ Missile-borne: high-temperature ablation, array thermal power consumption ⑤ Spaceborne: temperature gradient generated upon entering and leaving the earth shadow, space thermal radiation, array thermal power consumption
Main factors affecting antenna electrical performance	① Position offset, direction deflection and mutual coupling change of antenna elements due to array deformation ② Material properties and uneven thickness of the radome after high-temperature ablation ③ Element feed error: temperature drift of electronic device performance, power ripple, phase shifter quantification error
Application of SET coupling technology	① Establishment of SET coupling model based on the coupling relationship among structure, temperature, and electrical performance ② Influence of antenna fabrication accuracy on electric performance ③ Efficient heat dissipation design and comprehensive lightweight optimization design for optimum electrical performance ④ Sparse array design considering antenna radiation and scattering performance
Performance adjustment of APAA in service environment	① Layout of strain sensor for structural condition monitoring ② High-precision reconstruction of antenna array ③ Electrical performance compensation of APAA: compensation of digital quantification error, compensation method for radome-enclosed antenna, calculation method of excitation current compensation based on SET coupling ④ Key technology of performance compensation software for APAA

composites are widely used in aerospace because of their excellent mechanical properties, but their materials and fabrication processes are complicated. Based on the idea of SET coupling, the mapping relationship between monitoring data such as material stress and strain, equipment performance, and structural fatigue can be directly established to discover hidden characteristics of new materials.

5. Conclusion

APAA is an important electronic equipment to protect homeland security and plays an important role in achieving precise strike in military field. This paper summarizes the development trend of APAA on different platforms of land, sea, air, and space and lists the structural characteristics and performance parameters of APAAs. The harsh environment loads faced by various radars in modern five-dimensional battlefield environment and the effects of loads on APAA detection performance are analysed. The SET coupling theory of APAA is summarized, and the in-depth study is carried out from three aspects: array antenna structure error, high-temperature ablation of radome, and element feed error influence. The application of SET coupling model in antenna array design and manufacturing is summarized, and the correlation between antenna electromagnetic performance and antenna structure displacement field and temperature field is summarized, which provides theoretical basis for antenna designers and engineers. In order to ensure the reliable service of APAA under service load, the APAA in service is monitored and regulated in real time from three aspects: antenna array strain sensor layout, high-precision reconstruction of antenna array deformation, and compensation of antenna electrical performance. The main work is shown in Table 7. Finally, the future development trend of SET coupling technology is prospected.

Data Availability

The data used to support the findings of this study are available from the corresponding author upon reasonable request.

Conflicts of Interest

The authors declare that they have no conflicts of interest.

Acknowledgments

This study was supported by National Natural Science Foundation of China under grant nos. 51975447 and 52105272, National Key Research and Development Program of China under grant no. 2021YFC2203600, National Defense Basic Scientific Research Program of China under grant no. JCKY2021210B007, and Scientific Research Program Funded by Shaanxi Provincial Education Department under grant no. 21JK0721.

References

[1] E. Brookner, "Advances and breakthroughs in radars and phased-arrays," in *Proceedings of the 2016 CIE International Conference on Radar*, pp. 1–9, IEEE, Guangzhou, China, October 2016.

[2] V. Obukhovets, "Some new trends in phased antenna array designing," in *Proceedings of the Radiation and Scattering of Electromagnetic Waves*, pp. 20–23, IEEE, Divnomorskoe, Russia, June 2019.

[3] J. S. Herd and M. D. Conway, "The evolution to modern phased array architectures," *Proceedings of the IEEE*, vol. 104, no. 3, pp. 519–529, 2016.

[4] Y. Xiong and W. Xie, "Adaptive mutual coupling compensation method for airborne STAP radar with end-fire array," *IEEE Transactions on Aerospace and Electronic Systems*, vol. 58, no. 2, pp. 1283–1298, 2022.

[5] A. Fina, A. Di Carlofelice, and F. De Paulis, "High power, thermally efficient, X-band 3D T/R module with calibration capability for space radar," *IEEE Access*, vol. 6, pp. 60921–60929, 2018.

[6] R. Bil, M. Brandfass, and J. P. van Bezouwen, "Future technological challenges for high performance radar," in *Proceedings of the 19th International Radar Symposium (IRS)*, pp. 1–10, IEEE, Bonn, Germany, June, 2018.

[7] A. K. Mishra, "AESA radar and its application," in *Proceedings of the 2018 International Conference on Communication, Computing and Internet of Things (IC3IoT)*, pp. 205–209, IEEE, Chennai, India, February 2018.

[8] H. Liu, W. Wang, D. Tang, L. Zhang, Y. Wang, and E. Miao, "Thermal deformation modeling for phased array antenna compensation control," *Sensors*, vol. 22, no. 6, p. 2325, 2022.

[9] C. S. Wang, Y. Wang, J. Zhou, M. Wang, J. Zhong, and B. Duan, "Compensation method for distorted planar array antennas based on structural–electromagnetic coupling and fast Fourier transform," *IET Microwaves, Antennas and Propagation*, vol. 12, no. 6, pp. 954–962, 2018.

[10] S. Lou, W. Wang, H. Bao et al., "A compensation method for deformed array antennas considering mutual coupling effect," *IEEE Antennas and Wireless Propagation Letters*, vol. 17, no. 10, pp. 1900–1904, 2018.

[11] C. S. Wang, Y. Wang, S. Yuan et al., "A compensation method for active phased array antennas: using a strain-electromagnetic coupling model," *IEEE Antennas and Propagation Magazine*, vol. 63, no. 4, pp. 78–88, 2021.

[12] J. Zhou, L. Kang, B. Tang, B. Tang, J. Huang, and C. Wang, "Adaptive compensation of flexible skin antenna with embedded fiber Bragg grating," *IEEE Transactions on Antennas and Propagation*, vol. 67, no. 7, pp. 4385–4396, 2019.

[13] G. Y. Lu, J. Y. Zhou, G. P. Cai, G. Q. Fang, L. L. Lv, and F. J. Peng, "Studies of thermal deformation and shape control of a space planar phased array antenna," *Aerospace Science and Technology*, vol. 93, Article ID 105311, 2019.

[14] X. Wei, E. Miao, Y. Chen, and W. Wang, "Thermo-mechanical coupling modeling of active phased array antennas," *International Journal of Precision Engineering and Manufacturing*, vol. 20, no. 11, pp. 1893–1904, 2019.

[15] Z. Ma and X. Chen, "Strain transfer characteristics of surface-attached FBGs in aircraft wing distributed deformation measurement," *Optik*, vol. 207, Article ID 164468, 2020.

[16] C. S. Wang, Y. Wang, Y. Chen et al., "Coupling model and electronic compensation of antenna-radome system for hypersonic vehicle with effect of high-temperature ablation,"

IEEE Transactions on Antennas and Propagation, vol. 68, no. 3, pp. 2340–2355, 2020.

[17] L. Huo, G. Liao, Z. Yang, P. Huang, and J. Zhang, "An efficient error estimation method for antenna distortions in space based radar," *Digital Signal Processing*, vol. 89, pp. 8–16, 2019.

[18] G. Sa, Z. Liu, C. Qiu, and J. Tan, "Tolerance modeling and analysis considering form defects for spaceborne array antenna," *Applied Sciences*, vol. 10, no. 8, p. 2840, 2020.

[19] M. Alibakhshikenari, B. S. Virdee, L. Azpilicueta et al., "A comprehensive survey of "metamaterial transmission-line based antennas: design, challenges, and applications," *IEEE Access*, vol. 8, pp. 144778–144808, 2020.

[20] M. Alibakhshikenari, F. Babaeian, B. S. Virdee et al., "A comprehensive survey on "various decoupling mechanisms with focus on metamaterial and metasurface principles applicable to SAR and MIMO antenna systems," *IEEE Access*, vol. 8, pp. 192965–193004, 2020.

[21] M. Alibakhshikenari, E. M. Ali, M. Soruri et al., "A comprehensive survey on antennas on-chip based on metamaterial, metasurface, and substrate integrated waveguide principles for millimeter-waves and terahertz integrated circuits and systems," *IEEE Access*, vol. 10, pp. 3668–3692, 2022.

[22] I. Nadeem, M. Alibakhshikenari, F. Babaeian et al., "A comprehensive survey on "Circular Polarized Antennas"," for existing and emerging wireless communication technologies," *Journal of Physics D: Applied Physics*, vol. 55, no. 3, pp. 033002–033018, 2021.

[23] M. Alibakhshikenari, B. S. Virdee, C. H. See et al., "Dual-polarized highly folded bowtie antenna with slotted self-grounded structure for sub-6 GHz 5G applications," *IEEE Transactions on Antennas and Propagation*, vol. 70, no. 4, pp. 3028–3033, 2022.

[24] M. Alibakhshikenari, S. M. Moghaddam, and A. U. Zaman, "Wideband sub-6 GHz self-grounded bow-tie antenna with new feeding mechanism for 5G communication systems," in *Proceedings of the 13th European Conference on Antennas and Propagation (EuCAP)*, pp. 1–4, IEEE, Krakow, Poland, March 2019.

[25] Z. N. Chen, X. Qing, X. Tang, W. E. Liu, and R. Xu, "Phased array metantennas for satellite communications," *IEEE Communications Magazine*, vol. 60, no. 1, pp. 46–50, 2022.

[26] R. L. Haupt and Y. Rahmat-Samii, "Antenna array developments: a perspective on the past, present and future," *IEEE Antennas and Propagation Magazine*, vol. 57, no. 1, pp. 86–96, 2015.

[27] Z. Zhan, T. Xu, and S. Hu, "A KU band high integrated active phased array antenna for radar seeker," in *Proceedings of the IET International Radar Conference (IET IRC 2020)*, pp. 244–247, IET, Chongqing, China, November 2020.

[28] S. H. Talisa, K. W. O'Haver, T. M. Comberiate, M. D. Sharp, and O. F. Somerlock, "Benefits of digital phased array radars," *Proceedings of the IEEE*, vol. 104, no. 3, pp. 530–543, 2016.

[29] C. S. Wang, Y. Wang, P. Lian et al., "Space phased array antenna developments: a perspective on structural design," *IEEE Aerospace and Electronic Systems Magazine*, vol. 35, no. 7, pp. 44–63, 2020.

[30] R. Cui, J. Pan, and J. Zhu, "Research on jamming effect evaluation method of AN/TPY-2 radar using set pair approach degree," in *Proceedings of the International Conference on Artificial Intelligence, Information Processing and Cloud Computing*, pp. 1–5, ACM, Sanya, China, December, 2019.

[31] P. Podvig, "History and the current status of the Russian early-warning system," *Science and Global Security*, vol. 10, no. 1, pp. 21–60, 2002.

[32] Y. Otani, N. Kohtake, and Y. Ohkami, "Dual-Use system architecture for a space situational awareness system in Japan," in *Proceedings of the 2013 IEEE Aerospace Conference*, pp. 1–8, IEEE, Montana, MT USA, March, 2013.

[33] S. Dryer, E. Levine, and M. Peleg, "EL/M 2080 ATBM early warning and fire control radar system," in *Proceedings of the International Symposium on Phased Array Systems and Technology*, pp. 11–16, IEEE, Massachusetts, MA, USA, October, 1996.

[34] Z. Zhang, J. Wu, J. Dai, and C. He, "Optimal path planning with modified A-Star algorithm for stealth unmanned aerial vehicles in 3D network radar environment," *Proceedings of the Institution of Mechanical Engineers - Part G: Journal of Aerospace Engineering*, vol. 236, no. 1, pp. 72–81, 2022.

[35] D. K. Barton, "Radar today," *Microwave Journal*, vol. 48, no. 1, pp. 24–31, 2005.

[36] H. Fireman, J. Fowler, J. Mclntire, and C. J. Wilkins, "Lpd 17: in the midst of reform," *Naval Engineers Journal*, vol. 107, no. 3, pp. 267–282, 1995.

[37] M. R. Stiglitz and C. Blanchard, "Practical phased-array antenna systems," *Microwave Journal*, vol. 35, no. 3, pp. 168-169, 1992.

[38] W. J. Fontana and K. H. Krueger, "AN/SPY-3:The navy's next-generation force protection radar system," in *Proceedings of the IEEE International Symposium on Phased Array Systems and Technology*, pp. 594–603, IEEE, Massachusetts, MA, USA, October, 2003.

[39] K. W. O'Haver, C. K. Barker, and G. D. Dockery, "Radar development for air and missile defense," *Johns Hopkins APL Technical Digest*, vol. 34, no. 2, pp. 140–153, 2018.

[40] V. Machi and C. Lee, "3D modeling could speed procurement of navy destroyer," *National Defense*, vol. 102, no. 773, pp. 25–27, 2018.

[41] V. Chernyak, I. Y. Immoreev, and B. M. Vovshin, "Radar in the Soviet Union and Russia: a brief historical outline," *IEEE Aerospace and Electronic Systems Magazine*, vol. 18, no. 12, pp. 8–12, 2003.

[42] G. Dedden, "SMART-L multibeam radar," in *Proceedings of the First European Radar Conference*, pp. 17–20, IEEE, Amsterdam, Netherlands, October 2004.

[43] L. I. U. Guan-xin, "Influence of aircraft characteristics on radar detection and tracking," *Journal of Astronautic Metrology and Measurement*, vol. 38, no. 6, p. 63, 2018.

[44] H. Hommel, "Current status of airborne active phased array (AESA) radar systems and future trends," in *Proceedings of the First European Radar Conference*, pp. 121–124, IEEE, Amsterdam, Netherlands, October, 2004.

[45] T. Gao, Q. Wei, and P. Wang, "The development status and trend of airborne multifunctional radar," in *Proceedings of the 2021 IEEE International Conference on Artificial Intelligence and Industrial Design*, pp. 327–330, IEEE, Guangzhou, China, May, 2021.

[46] K. Zikidis, A. Skondras, and C. Tokas, "Low observable principles, stealth aircraft and anti-stealth technologies," *Journal of Computations and Modelling*, vol. 4, no. 1, pp. 129–165, 2014.

[47] N. MyERS, "The Russian Aerospace Force," *Security Forum*, Wydawnictwo Naukowe Akademii WSB, vol. 2 , pp. 91–103, 2018.

[48] G. Martin, "Fifth-generation fighter options," *Defence Review Asia*, vol. 14, no. 2, pp. 12–18, 2020.

[49] L. C. T. R. McCabe, "The limits of tactical aviation technology," *Air and Space Power Journal*, vol. 29, no. 5, pp. 91–98, 2015.

[50] X. Wang, "Review on polarimetric phased array radar technologies," *Radar Science and Technology*, vol. 19, no. 4, pp. 349–370, 2021.

[51] J. Drew, "Air force adding electronic protections: raytheon's new AIM-120d AMRAAM declared ready for battle," *Air Force Times*, vol. 26, no. 13, p. 7, 2015.

[52] P. Chaudhry, "Strength in diversity: the sukhoi-rafale duo," *Vayu Aerospace and Defence Review*, vol. 5, pp. 46–49, 2021.

[53] G. Franceschetti and R. Lanari, *Synthetic Aperture Radar Processing*, CRC Press, Boca Raton, FL, USA, 2018.

[54] A. H. M. Ng, L. Ge, Z. Du, S. Wang, and C. Ma, "Satellite radar interferometry for monitoring subsidence induced by longwall mining activity using Radarsat-2, Sentinel-1 and ALOS-2 data," *International Journal of Applied Earth Observation and Geoinformation*, vol. 61, pp. 92–103, 2017.

[55] G. Fornaro, F. Serafino, and D. Reale, "SAR tomography: application examples," in *Proceedings of the 8th European Conference on Synthetic Aperture Radar*, pp. 1-2, VDE, Aachen, Germany, June, 2010.

[56] L. Li, F. Zhang, Y. Shao, Q. Wei, Q. Huang, and Y. Jiao, "Airborne SAR radiometric calibration based on improved sliding window integral method," *Sensors*, vol. 22, no. 1, p. 320, 2022.

[57] E. J. Arnold, J. B. Yan, R. D. Hale, F. Rodriguez-Morales, and P. Gogineni, "Identifying and compensating for phase center errors in wing-mounted phased arrays for ice sheet sounding," *IEEE Transactions on Antennas and Propagation*, vol. 62, no. 6, pp. 3416–3421, 2014.

[58] T. Takahshi, N. Nakamoto, and M. Ohtsuka, "A simple onboard calibration method and its accuracy for mechanical distortions of satellite phased array antennas," in *Proceedings of the 3rd European Conference on Antennas and Propagation*, pp. 1573–1577, IEEE, Berlin, Germany, June, 2009.

[59] H. S. C. Wang, "Performance of phased-array antennas with mechanical errors," *IEEE Transactions on Aerospace and Electronic Systems*, vol. 28, no. 2, pp. 535–545, 1992.

[60] A. Ossowska, J. H. Kim, and W. Wiesbeck, "Influence of mechanical antennas distortions on the performance of the HRWS SAR system," in *Proceedings of the 2007 IEEE International Geoscience and Remote Sensing Symposium*, pp. 2152–2155, IEEE, Barcelona Spain, January, 2017.

[61] M. Alibakhshikenari, B. S. Virdee, and E. Limiti, "Study on isolation and radiation behaviours of a 34× 34 array-antennas based on SIW and metasurface properties for applications in terahertz band over 125–300 GHz," *Optik*, vol. 206, Article ID 163222, 2020.

[62] M. Alibakhshikenari, B. S. Virdee, P. Shukla et al., "Isolation enhancement of densely packed array antennas with periodic MTM-photonic bandgap for SAR and MIMO systems," *IET Microwaves, Antennas and Propagation*, vol. 14, no. 3, pp. 183–188, 2020.

[63] M. Alibakhshikenari, B. S. Virdee, C. H. See, R. A. Abd-Alhameed, F. Falcone, and E. Limiti, "Surface wave reduction in antenna arrays using metasurface inclusion for MIMO and SAR systems," *Radio Science*, vol. 54, no. 11, pp. 1067–1075, 2019.

[64] M. Alibakhshikenari, M. Khalily, B. S. Virdee, C. H. See, R. A. Abd-Alhameed, and E. Limiti, "Mutual-coupling isolation using embedded metamaterial EM bandgap decoupling slab for densely packed array antennas," *IEEE Access*, vol. 7, pp. 51827–51840, 2019.

[65] M. Alibakhshikenari, M. Khalily, B. S. Virdee, C. H. See, R. A. Abd-Alhameed, and E. Limiti, "Mutual coupling suppression between two closely placed microstrip patches using EM-bandgap metamaterial fractal loading," *IEEE Access*, vol. 7, pp. 23606–23614, 2019.

[66] M. Alibakhshikenari, B. S. Virdee, P. Shukla et al., "Interaction between closely packed array antenna elements using meta-surface for applications such as MIMO systems and synthetic aperture radars," *Radio Science*, vol. 53, no. 11, pp. 1368–1381, 2018.

[67] M. Alibakhshikenari, B. S. Virdee, P. Shukla et al., "Antenna mutual coupling suppression over wideband using embedded periphery slot for antenna arrays," *Electronics*, vol. 7, no. 9, p. 198, 2018.

[68] M. Alibakhshikenari, B. S. Virdee, C. H. See et al., "Study on isolation improvement between closely-packed patch antenna arrays based on fractal metamaterial electromagnetic bandgap structures," *IET Microwaves, Antennas and Propagation*, vol. 12, no. 14, pp. 2241–2247, 2018.

[69] M. Alibakhshikenari, P. Shukla, B. S. Virdee et al., "Metasurface wall suppression of mutual coupling between microstrip patch antenna arrays for THz-band applications," *Progress in Electromagnetics Research Letters*, vol. 75, pp. 105–111, 2018.

[70] A. A. Althuwayb, "Low-interacted multiple antenna systems based on metasurface-inspired isolation approach for MIMO applications," *Arabian Journal for Science and Engineering*, vol. 47, no. 3, pp. 2629–2638, 2022.

[71] H. S. Farahani, M. Veysi, M. Kamyab, and A. Tadjalli, "Mutual coupling reduction in patch antenna arrays using a UC-EBG superstrate," *IEEE Antennas and Wireless Propagation Letters*, vol. 9, pp. 57–59, 2010.

[72] O. G. Vendik, D. S. Kozlov, and M. D. Parnes, "Influence of mutual coupling and current distribution errors on advanced phased antenna array nulling synthesis," *Open Journal of Antennas and Propagation*, vol. 1, no. 3, p. 35, 2013.

[73] Y. Zhang and L. Zhang, "Tolerances of optimum thining linear arrays," *Journal of Xidian University*, vol. 1, pp. 30–40, 1992.

[74] M. Mohammadi Shirkolaei, H. R. Dalili Oskouei, and M. Abbasi, "Design of 1* 4 microstrip antenna array on the human thigh with gain enhancement," *IETE Journal of Research*, vol. 2021, pp. 1–7, 2021.

[75] Q. Bai, H. J. Lee, and K. L. Ford, "Switchable textile microstrip antenna for on/off-body communications and shape distortion study," in *Proceedings of the 2012 IEEE Asia-Pacific Conference on Antennas and Propagation*, pp. 114-115, IEEE, Singapore, August, 2012.

[76] J. P. Geng, J. Li, R. H. Jin, S. Ye, X. Liang, and M. Li, "The development of curved microstrip antenna with defected ground structure," *Progress in Electromagnetics Research*, vol. 98, pp. 53–73, 2009.

[77] B. I. Wu and I. Ehrenberg, "Ultra conformal patch antenna array on a doubly curved surface," in *Proceedings of the 2013 IEEE International Symposium on Phased Array Systems and Technology*, pp. 729–798, IEEE, Massachusetts, MA USA, October, 2013.

[78] R. Han, *Analysis of Electronical Performances of Spaceborne Microstrip Array Antenna with Thermal Deformation*Xidian University, Xi'an, China, 2014.

[79] M. Kang, *Coupled Structural-Electromagnetic-Thermal Modelling, Error Analysis and Optimization Design of*

*Active Phased Array Antennas*Xidian University, Xi'an, China, 2017.

[80] Y. Wang, *Electromechanical Coupling Analysis and Performance Compensation of Active Phased Array Antennas in Operating Environment*Xidian University, Xi'an, China, 2019.

[81] C. Wang, *Electromechanical Coupling Analysis, Design and Compensation of Active Phased Array Antennas*Science Press, Beijing, China, 2021.

[82] Y. J. Qin and J. G. He, "Analysis of tangent oval radome based on Matlab," in *Proceedings of the Asia-Pacific Microwave Conference Proceedings*, pp. 3–6, IEEE, Suzhou China, December, 2005.

[83] L. B. Weckesser, "Radome aerodynamic heating effects on boresight error," in *Proceedings of the 15th Symposium on Electromagnetic Windows*, pp. 97–101, Proceedings, Atlanta, GA, USA, June, 1980.

[84] R. U. N. Parul and R. M. Jha, "Temperature dependent EM performance predictions of dielectric slab based on inhomogeneous planar layer model," in *Proceedings of the IEEE International Symposium on Antennas and Propagation*, pp. 1-2, IEEE, Chicago, IL, USA, July 2012.

[85] R. U. Nair and R. M. Jha, "Electromagnetic design and performance analysis of airborne radomes: trends and perspectives [antenna applications corner]," *IEEE Antennas and Propagation Magazine*, vol. 56, no. 4, pp. 276–298, 2014.

[86] L. Zhong, G. Fu, and J. Lu, "A research for influence of temperature on T/R module in radar," in *Proceedings of the IEEE Prognostics and System Health Management Conference*, pp. 1–9, IEEE, Beijing, China, October, 2015.

[87] Q. Yang, *Analysis on the Effect of Temperature on Electrical Properties of Microwave Transmit/Receive Modules' Key Components*Xidian University, Xi'an, China, 2014.

[88] M. Mohammadi Shirkolaei and J. Ghalibafan, "Magnetically scannable slotted waveguide antenna based on the ferrite with gain enhancement," *Waves in Random and Complex Media*, vol. 2021, pp. 1–11, 2021.

[89] M. Masoumi, H. R. Dalili Oskouei, M. Mohammadi Shirkolaei, and A. R. Mirtaheri, "Substrate integrated waveguide leaky wave antenna with circular polarization and improvement of the scan angle," *Microwave and Optical Technology Letters*, vol. 64, no. 1, pp. 137–141, 2022.

[90] F. Moayyed, H. R. Dalili Oskouei, and M. Mohammadi Shirkolaei, "High gain and wideband multi-stack multilayer anisotropic dielectric antenna," *Progress In Electromagnetics Research Letters*, vol. 99, pp. 103–109, 2021.

[91] M. Mohammadi Shirkolaei, "A new design approach of low-noise stable broadband microwave amplifier using hybrid optimization," *IETE Journal of Research*, vol. 2020, pp. 1–7, 2021.

[92] M. Mohammadi, "Modal analysis of directional coupler and its equivalent circuit," *Advanced Electromagnetics*, vol. 8, no. 4, pp. 103–107, 2019.

[93] M. Mohammadi, F. H. Kashani, and J. Ghalibafan, "A compact planar monopulse combining network at W-band," in *Proceedings of the 5th IEEE GCC Conference and Exhibition*, pp. 1–5, IEEE, Kuwait City, Kuwait, March, 2009.

[94] P. Wang, "The effects of power supply ripple on PD radar performance," *Modern Radar*, vol. 19, no. 4, pp. 79–87, 1997.

[95] K. S. Wong and G. F. Ricciardi, "Characterization of amplitude modulation bias coupling for solid-state high-power amplifiers," in *Proceedings of the IEEE International Symposium on Phased Array Systems and Technology*, pp. 64–68, IEEE, Waltham, MA, USA, October, 2013.

[96] D. K. Abe, D. E. Pershing, K. T. Nguyen, R. E. Myers, F. N. Wood, and B. Levush, "Experimental study of phase pushing in a fundamental-mode multiple-beam klystron," *IEEE Transactions on Electron Devices*, vol. 54, no. 5, pp. 1253–1258, 2007.

[97] K. Yang, "Effect of power supply ripple on noise performance of low noise amplifiers," *Wireless Communication Technology*, vol. 6, no. 1, pp. 45–47, 1997.

[98] Z. Wei, "The effects of the pulse modulation shape distortion and the power supply ripple on the radar transmitter performance," *Modern Radar*, vol. 14, no. 3, pp. 81–91, 1992.

[99] W. Zhang, "Research into power-supply ripple affects TWT amplifier," *Vacuum Electronics*, vol. 4, pp. 58–61, 2014.

[100] X. Tan, W. Wu, and H. Sun, "Analyzing the Effect of Power Supply Ripple on the Performance of Chirp Radar," *Radio Engineering*, vol. 1, pp. 75–77, 2001.

[101] H. Kamoda, J. Tsumochi, T. Kuki, and F. Suginoshita, "A study on antenna gain degradation due to digital phase shifter in phased array antennas," *Microwave and Optical Technology Letters*, vol. 53, no. 8, pp. 1743–1746, 2011.

[102] T. Gao, "Influence of phase quantization on peak sidelobe level of phased array antenna," *Chinese Space Science Technology*, vol. 1, pp. 14–19, 1994.

[103] Z. L. Liu, Y. C. Guo, and G. Y. Zhang, "Appropriate random phasing techniques to reduce phase quantization side-lobes in phased array antennas," *Journal of Microwaves*, vol. 4, pp. 53–55, 2008.

[104] Z. Yang, "The analysis in offset of antenna pattern with monte-carlo method," *Journal of Projectiles, Rockets, Missiles and Guidance*, pp. 353-354, 2005.

[105] Z. Feng, Z. Fang, Z. Wei, X. Chen, Z. Quan, and D. Ji, "Joint radar and communication: a survey," *China Communications*, vol. 17, no. 1, pp. 1–27, 2020.

[106] L. V. Blake, "Recent advancements in basic radar range calculation technique," *Ire Transactions on Military Electronics*, vol. 5, no. 2, pp. 154–164, 1961.

[107] M. I. Skolnik, *An Introduction to Impulse Radar*, Naval Research Lab Report, Washington DC, USA, 1990.

[108] L. E. Brennan and I. S. Reed, "Optimum processing of unequally spaced radar pulse trains for clutter rejection," *IEEE Transactions on Aerospace and Electronic Systems*, vol. 4, no. 3, pp. 474–477, 1968.

[109] J. D. Glass, *Monopulse Processing and Tracking of Maneuvering Targets*, Georgia Institute of Technology, Atlanta, GA, USA, 2015.

[110] J. K. Hsiao, "Design of error tolerance of a phased array," *Electronics Letters*, vol. 21, no. 19, pp. 834–836, 1985.

[111] J. Xiu, *Mechanical -Electromagnetic Coupling Modeling and Optimization Design of Radar Structural Deformation and Detection Performance*Xidian University, Xi'an, China, 2019.

[112] A. A. Eldek, "Ultrawideband double rhombus antenna with stable radiation patterns for phased array applications," *IEEE Transactions on Antennas and Propagation*, vol. 55, no. 1, pp. 84–91, 2007.

[113] B. Lu, S. X. Gong, S. Zhang, Y. Guan, and J. Ling, "Optimum spatial arrangement of array elements for suppression of grating-lobes of radar cross section," *IEEE Antennas and Wireless Propagation Letters*, vol. 9, no. 9, pp. 114–117, 2010.

[114] N. Yuan, T. S. Yeo, X. C. Nie, and L. Wei, "A fast analysis of scattering and radiation of large microstrip antenna arrays," *IEEE Transactions on Antennas and Propagation*, vol. 51, no. 9, pp. 2218–2226, 2003.

[115] T. Tanaka, Y. Nishioka, and Y. Inasawa, "MoM analysis of radiation and scattering of broadband array Antenna," in

Proceedings of the 2013 International Symposium on Electromagnetic Theory, pp. 804–807, IEEE, Hiroshima, Japan, May, 2013.

[116] Y. Chi, P. L. Zhang, and G. Y. Chen, "Pattern synthesis based on immune clone selection algorithm," *Communications Technology*, vol. 42, no. 5, pp. 71–74, 2009.

[117] W. Wang, *Coupling Structural-RCS Modeling and Integration Performance Analysis for Array Antennas with Mechanical Distortion*Xidian University, Xi'an, China, 2014.

[118] L. Su, L. Zhi, and J. Liu, "Analysis and control of large phased-array radar antenna array structure precision," *Fire Control Radar Technology*, vol. 46, no. 02, pp. 75–79, 2017.

[119] X. Hu, M. Kang, and W. Wang, "On influence of structural errors for hexagonal phased array antennas," *Journal of Beijing University of Aeronautics and Astronautics*, vol. 39, no. 12, pp. 1629–1632, 2013.

[120] E. Zaitsev and J. Hoffman, "Phased array flatness effects on antenna system performance," in *Proceedings of the 2010 IEEE International Symposium on Phased Array Systems and Technology*, pp. 121–125, IEEE, Waltham, IL, USA, October, 2010.

[121] B. H. Liu, C. H. Cheng, and H. P. Yuan, "Analysis and research of effect factor and measurement of radar structure precision," *Electro-Mechanical Engineering*, vol. 35, no. 01, pp. 5–10, 2019.

[122] A. A. Althuwayb, "On-chip antenna design using the concepts of metamaterial and SIW principles applicable to terahertz integrated circuits operating over 0.6-0.622 THz," *International Journal of Antennas and Propagation*, vol. 2020, no. 9, Article ID 6653095, 9 pages, 2020.

[123] A. A. Althuwayb, "MTM-and SIW-inspired bowtie antenna loaded with AMC for 5G mm-wave applications," *International Journal of Antennas and Propagation*, vol. 2021, no. 9, Article ID 6658819, 7 pages, 2021.

[124] A. A. Althuwayb, "Enhanced radiation gain and efficiency of a metamaterial-inspired wideband microstrip antenna using substrate integrated waveguide technology for sub-6 GHz wireless communication systems," *Microwave and Optical Technology Letters*, vol. 63, no. 7, pp. 1892–1898, 2021.

[125] M. Mobrem, "Methods of analyzing surface accuracy of large antenna structures due to manufacturing tolerances," in *Proceedings of the 44th AIAA/ASME/ASCE/AHS/ASC Structures, Structural Dynamics, and Materials Conference*, p. 1453, ARC, Norfolk, VA, USA, April, 2013.

[126] Q. Cui, M. Li, and Z. Peng, "Configuration optimization and surface accuracy investigation of solid surface deployable reflector," *Theory, Methodology, Tools and Applications for Modeling and Simulation of Complex Systems*, pp. 672–684, Springer, Singapore, 2016.

[127] H. D. He, X. Wei, and S. P. Yang, "Error analysis of admittance of radiating slot in planar slotted-waveguide array antennas with Monte Carlo method," *Journal of Radio Wave Science*, vol. 24, no. 2, pp. 365–368, 2009.

[128] L. Fan, "Multi-objective optimization design method of satellite antenna reflector," in *Proceedings of the 21st National Composite Materials Academic Conference(NCCM-21)*, pp. 116–122, Hohhot, China, August, 2020.

[129] M. Alibakhshikenari, B. S. Virdee, S. Salekzamankhani et al., "High-isolation antenna array using SIW and realized with a graphene layer for sub-terahertz wireless applications," *Scientific Reports*, vol. 11, no. 1, pp. 10218–10314, 2021.

[130] M. Alibakhshikenari, B. S. Virdee, A. A. Althuwayb et al., "Study on on-chip antenna design based on metamaterial-inspired and substrate-integrated waveguide properties for millimetre-wave and THz integrated-circuit applications," *Journal of Infrared, Millimeter and Terahertz Waves*, vol. 42, no. 1, pp. 17–28, 2021.

[131] M. Alibakhshikenari, B. S. Virdee, M. Khalily et al., "High-gain on-chip antenna design on silicon layer with aperture excitation for terahertz applications," *IEEE Antennas and Wireless Propagation Letters*, vol. 19, no. 9, pp. 1576–1580, 2020.

[132] M. Alibakhshikenari, B. S. Virdee, C. H. See et al., "Study on improvement of the performance parameters of a novel 0.41-0.47 THz on-chip antenna based on metasurface concept realized on 50 μm GaAs-layer," *Scientific Reports*, vol. 10, no. 1, pp. 11034–11039, 2020.

[133] M. Alibakhshikenari, B. S. Virdee, C. H. See, R. A. Abd-Alhameed, F. Falcone, and E. Limiti, "High-gain metasurface in polyimide on-chip antenna based on CRLH-TL for sub-terahertz integrated circuits," *Scientific Reports*, vol. 10, no. 1, pp. 4298-4299, 2020.

[134] S. Zhang, S. X. Gong, and B. Lu, "Optimizing both radiation and scattering characteristics of the array antenna utilizing PSO," *Journal of Xidian University*, vol. 37, no. 4, pp. 726–730, 2010.

[135] W. Wang, S. Gong, X. Wang, Y. Guan, and W. Jiang, "Differential evolution algorithm and method of moments for the design of low-RCS antenna," *IEEE Antennas and Wireless Propagation Letters*, vol. 9, pp. 295–298, 2010.

[136] L. Cong, "A broadband high-gain low-RCS mushroom antenna using Anisotropic Metasurface," in *Proceedings of the 2018 National Microwave and Millimeter Wave Conference*, pp. 350–353, Chengdu China, May, 2018.

[137] G. Zhang, *Space Detection Phased Array Radar*Science Press, Beijing, China, 2001.

[138] X. Zhang, *Design and Heat Dissipation Characteristics Study of LTCC Microchannels Served to Power Amplifier Chip Modules*University of Electronic Science and Technology of China, Chengdu, China, 2017.

[139] M. Scott, "Sampson MFR active phased array antenna," in *Proceedings of the IEEE International Symposium on Phased Array Systems and Technology*, pp. 119–123, IEEE, Boston, MA, USA, October, 2003.

[140] H. Kawasaki, H. Noda, and T. Yabe, "Characteristics of reservoir embedded loop heat pipe in deployable radiator on ETS-VIII at beginning of the experiment under orbital environment," in *Proceedings of the 40th Thermophysics Conference*, p. 119, ARC, Seattle, WA, USA, June, 2008.

[141] W. Zhu, "Research on new type refrigeration device based on thermoelectric effect," *Smart Grid*, vol. 3, no. 09, pp. 823–828, 2015.

[142] Y. Hui, *Research on the Indirect Liquid Cooling Technique Based on Microchannels*Harbin Institute of Technology, Harbin, China, 2013.

[143] C. S. Wang, Z. M. Song, and M. K. Kang, "Application of micro-channel cold plate to active phased array antenna," *Electro-Mechanical Engineering*, vol. 1, p. 5, 2013.

[144] T. Lu, *Research on Equivalent Modeling Method of Heat Flow Characteristics of Microchannel of Phased Array Antenna and Thermal Design*University of Electronic Science and Technology of China, Chengdu, China, 2017.

[145] K. Matin, A. Bar-Cohen, and J. J. Maurer, "Modeling and simulation challenges in embedded two phase cooling: DARPA's ICECool program," in *Proceedings of the International Electronic Packaging Technical Conference and Exhibition*, vol. 56901, p. V003T10A024, ASME, San Francisco, CA, USA, November, 2015.

[146] R. Van Erp, R. Soleimanzadeh, L. Nela, G. Kampitsis, and E. Matioli, "Co-designing electronics with microfluidics for more sustainable cooling," *Nature*, vol. 585, pp. 211–216, 2020.

[147] J. Zhang, "Light-weighting technologies for the active phased array of spaceborne radar," in *Proceedings of the China Antenna Annual Conference*, pp. 14–10, CIE, Chengdu China, October 2009.

[148] M. Xu, "Design and fabrication of membrane active phased-array antennas," in *Proceedings of the China Antenna Annual Conference*, pp. 580–582, CIE, Xian China, October, 2017.

[149] J. Huang, "The development of inflatable array antennas," *IEEE Antennas and Propagation Magazine*, vol. 43, no. 4, pp. 44–50, 2001.

[150] M. S. Hauhe and J. J. Wooldridge, "High Density Packaging of X-band active array modules," *IEEE Transactions on Components Packaging and Manufacturing Technology Part A B*, vol. 20, no. 3, pp. 279–291, 1997.

[151] X. K. Wang, J. Yuan, and Z. X. Xiong, "Pattern synthesis of thinned linear arrays based on time modulated technique," *Journal of Shaanxi University of Technology(Natural Science Edition)*, vol. 34, no. 06, pp. 51–58, 2018.

[152] G. Ren, *Wideband DOA Estimation under Clutter Using MIMO Radar with Sparse Array*University of Electronic Science and Technology of China, Chengdu, China, 2020.

[153] S. Q. Tang, *Radar Array and Pattern Optimization Design Based on Scene Requirements*University of Electronic Science and Technology of China, Chengdu, China, 2020.

[154] A. A. Khan and A. K. Brown, "Null steering in irregularly spaced sparse antenna arrays using aperture distributed subarrays and hybrid optimiser," *IET Microwaves, Antennas and Propagation*, vol. 8, no. 2, pp. 86–92, 2014.

[155] Z. W. Yang, S. He, and G. S. Liao, "Sensor position estimation for wing conformal antenna array," *Acta Electronica Sinica*, vol. 41, no. 10, pp. 1969–1974, 2013.

[156] G. Oliveri and A. Massa, "Genetic algorithm (GA)-enhanced almost difference set (ADS)-based approach for array thinning," *IET Microwaves, Antennas and Propagation*, vol. 5, no. 3, pp. 305–315, 2011.

[157] L. J. Li, B. H. Wang, and C. H. Xia, "Synthesis of sparse conformal array antennas pattern," *Acta Electronica Sinica*, vol. 45, no. 1, p. 8, 2017.

[158] E. T. Lee and H. C. Eun, "Optimal sensor placement in reduced-order models using modal constraint conditions," *Sensors*, vol. 22, no. 2, p. 589, 2022.

[159] C. He, J. Xing, J. Li, Q. Yang, R. Wang, and X. Zhang, "A combined optimal sensor placement strategy for the structural health monitoring of bridge structures," *International Journal of Distributed Sensor Networks*, vol. 9, no. 11, Article ID 820694, 2013.

[160] T. H. Yi and H. N. Li, "Methodology developments in sensor placement for health monitoring of civil infrastructures," *International Journal of Distributed Sensor Networks*, vol. 8, no. 8, Article ID 612726, 2012.

[161] B. Li and A. Der Kiureghian, "Robust optimal sensor placement for operational modal analysis based on maximum expected utility," *Mechanical Systems and Signal Processing*, vol. 75, pp. 155–175, 2016.

[162] R. Castro-Triguero, E. I. Saavedra Flores, F. A. Diazdelao, M. I. Friswell, and R. Gallego, "Optimal sensor placement in timber structures by means of a multi-scale approach with material uncertainty," *Structural Control and Health Monitoring*, vol. 21, no. 12, pp. 1437–1452, 2014.

[163] L. Vincenzi and L. Simonini, "Influence of model errors in optimal sensor placement," *Journal of Sound and Vibration*, vol. 389, pp. 119–133, 2017.

[164] T. Kim, B. D. Youn, and H. Oh, "Development of a stochastic effective independence (SEFI) method for optimal sensor placement under uncertainty," *Mechanical Systems and Signal Processing*, vol. 111, pp. 615–627, 2018.

[165] C. Papadimitriou and G. Lombaert, "The effect of prediction error correlation on optimal sensor placement in structural dynamics," *Mechanical Systems and Signal Processing*, vol. 28, pp. 105–127, 2012.

[166] C. Yang, K. Liang, and X. P. Zhang, "Strategy for sensor number determination and placement optimization with incomplete information based on interval possibility model and clustering avoidance distribution index," *Computer Methods in Applied Mechanics and Engineering*, vol. 366, Article ID 113042, 2020.

[167] S. Yuan, M. Yan, and J. Zhang, "Shape reconstruction method of spar wing structure," *Journal of Nanjing University of Aeronautics and Astronautics*, vol. 46, no. 6, pp. 825–830, 2014.

[168] M. Alioli, P. Masarati, M. Morandini, T. Carpenter, N. B. Osterberg, and R. Albertani, "Membrane shape and load reconstruction from measurements using inverse finite element analysis," *AIAA Journal*, vol. 55, no. 1, pp. 297–308, 2017.

[169] R. Bruno, N. Toomarian, and M. Salama, "Shape estimation from incomplete measurements: a neural-net approach," *Smart Materials and Structures*, vol. 3, no. 2, pp. 92–97, 1999.

[170] F. Li, *Research on Structural Response Reconstruction Method of Active Phased Array Antenna*Xidian University, Xi'an, China, 2018.

[171] M. Zhai, *Array Antenna Theory Guide*National Defense Industry Press, Arlington, Virginia, 2010.

[172] Z. L. Zhang, "Phase error analysis and compensation in airborne phased-array radar," *Radar Science and Technology*, vol. 35, no. 2, pp. 34–37, 2010.

[173] C. Wang, *A Determination Method of Amplitude and Phase Compensation of Deformed Active Phased Array Antenna for Digital Device Quantization*, Intellectual Property Publishing House, Beijing, China, 2017.

[174] Y. Zhou, *Software of Electrical Performance Calculation, Compensation and Integrated Design of Active Phased Array Antenna Orientated Structural-Electromagnetic Coupling*Xidian University, Xi'an, China, 2018.

[175] D. P. Yang, L. B. Wei, and Y. I. Shang-Jun, "Analysis and improvement of phase error effect on phase array antenna," *Radio Engineering*, vol. 43, no. 3, pp. 24–26, 2013.

[176] N. Hu, "Synthetic design of structure and adjustment mechanism of large phased array antennas," *Journal of Mechanical Engineering*, vol. 51, no. 1, p. 196, 2015.

[177] S. H. Son, J. S. Yun, and U. H. Park, "Theoretical analysis for beam pointing accuracy of stair-planar phased array antenna with tracking beam," in *Proceedings of the IEEE Antennas and Propagation Society International Symposium*, vol. 4, pp. 204–207, IEEE, Columbus, USA, June, 2003.

[178] G. Song, B. Kelly, and B. N. Agrawal, "Active position control of a shape memory alloy wire actuated composite beam," *Smart Materials and Structures*, vol. 9, no. 5, pp. 711–716, 2000.

[179] R. J. Mailloux, *Phased Array Antenna Brochure*, Publishing House of Electronics Industry, Beijing, China, 2007.

[180] T. Takano, H. Hosono, and K. Saegusa, "Proposal of a multiple folding phased array antenna and phase

compensation for panel steps," in *Proceedings of the 2011 IEEE International Symposium on Antennas and Propagation*, pp. 1557–1559, IEEE, Spokane, DC, USA, July, 2011.

[181] S. H. Son, S. Y. Eom, S. I. Jeon, and W. Hwang, "Automatic phase correction of phased array antennas by a genetic algorithm," *IEEE Transactions on Antennas and Propagation*, vol. 56, no. 8, pp. 2751–2754, 2008.

[182] M. Steyskal and R. J. Mailloux, "Generalization of a phased array error correction method," in *Proceedings of the IEEE Antennas and Propagation Society International Symposium*, pp. 506–509, IEEE, Baltimore ,MD, USA, July, 1996.

[183] G. Lesueur, D. Caer, and T. Merlet, "Active compensation techniques for deformable phased array antenna," in *Proceedings of the 3rd European Conference on Antennas and Propagation*, pp. 1578–1581, IEEE, Berlin Germany, June 2009.

[184] H. Schippers, J. H. Van Tongeren, and P. Knott, "Vibrating antennas and compensation techniques research in NATO/RTO/SET 087/RTG 50," in *Proceedings of the Aerospace Conference*, pp. 1–13, IEEE, Big Sky, USA, March, 2007.

[185] N. Appannagarri, I. Bardi, and R. Edlinger, "Modeling phased array antennas in Ansoft HFSS," in *Proceedings of the 2000 IEEE International Conference on Phased Array Systems and Technology*, pp. 323–326, IEEE, Dana Point, USA, May 2000.

[186] M. Rütschlin and T. Wittig, "State of the art antenna simulation with CST STUDIO SUITE," in *Proceedings of the 2015 9th European Conference on Antennas and Propagation*, pp. 1–5, IEEE, Lisbon, Portugal, April, 2015.

[187] C. Wei and K. L. Wu, "Array-antenna decoupling surfaces for quasi-yagi antenna arrays," in *Proceedings of the 2017 IEEE International Symposium on Antennas and Propagation and USNC/URSI National Radio Science Meeting*, pp. 2103-2104, IEEE, San Diego, CA, USA, July, 2017.

[188] C. Blair, S. L. Ruiz, and M. Morales, "A MultiPhysics simulation vision from antenna element design to systems link analysis," in *Proceedings of the 2019 International Conference on Electromagnetics in Advanced Applications*, pp. 1420–1422, IEEE, Granada Spain, October, 2019.

[189] A. Kedar, A. S. Bisht, and K. Sreenivasulu, "GaN based wide band C-band active phased array antenna design with wide scan volume," in *Proceedings of the 2020 IEEE International Radar Conference*, pp. 88–93, IEEE, Washington, DC, USA, April, 2020.

[190] J. Che, *Mechanical -Electromagnetic Coupling Modeling and Optimization Design of Radar Structural Deformation and Detection Performance*Xidian University, Xi'an, China, 2020.

[191] R. Xu, S. Gao, B. S. Izquierdo et al., "A review of broadband low-cost and high-gain low-terahertz antennas for wireless communications applications," *IEEE Access*, vol. 8, pp. 57615–57629, 2020.

[192] Y. He, Y. Chen, L. Zhang, S. W. Wong, and Z. N. Chen, "An overview of terahertz antennas," *China Communications*, vol. 17, no. 7, pp. 124–165, 2020.

[193] R. Kumar, P. K. Verma, and M. V. Kartikeyan, "Wide scanned electronically steered conformal active phased array antenna for Ku-band SATCOM," *International Journal of Microwave and Wireless Technologies*, vol. 11, no. 4, pp. 376–381, 2019.

[194] S. M. Baek, S. J. Lim, M. G. Ko, M. Y. Park, and M. S. Kim, "Structural design, fabrication and static testing of smart composite skin structure: conformal load-bearing SATCOM array antenna structure (CLSAAS)," *International Journal of Aeronautical and Space Sciences*, vol. 21, no. 1, pp. 50–62, 2020.

[195] Y. A. Huang, C. Zhu, W. N. Xiong et al., "Flexible smart sensing skin for "Fly-by-Feel" morphing aircraft," *Science China Technological Sciences*, vol. 65, pp. 1–29, 2021.

[196] M. R. Karim, X. Yang, and M. F. Shafique, "On chip antenna measurement: a survey of challenges and recent trends," *IEEE Access*, vol. 6, pp. 20320–20333, 2018.

[197] R. Karim, A. Iftikhar, B. Ijaz, and I. Ben Mabrouk, "The potentials, challenges, and future directions of on-chip-antennas for emerging wireless applications—a comprehensive survey," *IEEE Access*, vol. 7, pp. 173897–173934, 2019.

[198] R. Karim and P. Malcovati, "On-chip-antennas: next milestone in the big world of small satellites—a survey of potentials, challenges, and future directions," *IEEE Aerospace and Electronic Systems Magazine*, vol. 36, no. 1, pp. 46–60, 2021.